2-1-2016

THE EFFECT OF BIOFILM CARRIER LENGTH ON NITRIFICATION IN MOVING BED BIOFILM REACTORS: AN EXAMINATION OF MIXING INTENSITY, SHOCK LOADINGS, AND PH CHANGES

Kody Garcia

Follow this and additional works at: https://digitalrepository.unm.edu/ce_etds

Kody A. Garcia

_____
Candidate

Civil Engineering

_____
Department

This thesis is approved, and it is acceptable in quality and form for publication:

Approved by the Thesis Committee:

Andrew J. Schuler, Chairperson

_____

Kerry Howe

_____

José M. Cerrato

_____

THE EFFECT OF BIOFILM CARRIER LENGTH ON NITRIFICATION IN
MOVING BED BIOFILM REACTORS: AN EXAMINATION OF MIXING
INTENSITY, SHOCK LOADINGS, AND PH CHANGES

by

KODY A. GARCIA

B.S. EARTH AND PLANETARY SCIENCES

THESIS

Submitted in Partial Fulfillment of the

Requirements for the Degree of

Master of Science

Civil Engineering

The University of New Mexico

Albuquerque, New Mexico

December 2015

ACKNOWLEDGMENTS

I would like to thank Dr. Schuler, my advisor and committee chair, for the guidance and assistance in completing this study, and for the detailed teaching in both the classroom and in professional writing. His education will guide me in my career and allow me to be successful as I begin my engineering career outside of academia.

I also wish thank committee members, Dr. Howe and Dr. Cerrato, for their continued advice and recommendations through the duration of this study. Additionally, I want thank Dr. Howe and Dr. Cerrato for their thorough teaching methods in the classroom which will stick with me throughout my career.

I want to express immense gratitude to The Center for Water and the Environment: Center of Research Excellence in Science and Technology through the National Science Foundation for funding this project and for covering tuition expenses in my master's program.

Lastly, I must thank my family, my friends, and my pets for their seemingly limitless understanding and support of me and my aspirations.

THE EFFECT OF BIOFILM CARRIER LENGTH ON NITRIFICATION IN MOVING BED BIOFILM REACTORS: AN EXAMINATION OF MIXING INTENSITY, SHOCK LOADINGS, AND PH CHANGES

by

Kody A. Garcia

B.S., Earth and Planetary Sciences, University of New Mexico, 2012

M.S, Civil Engineering, University of New Mexico, 2015

ABSTRACT

Biofilms grown on free-floating attachment surfaces, as in integrated fixed film activated sludg (IFAS) and moving bed bioreactors (MBBRs) are commonly used in wastewater treatment, but little is known about how media geometry affects the biofilms and process performance. The objective of this study was to compare nitrification and growth of biofilms grown on different length media in bench-scale MBBRs. The carriers were cut from high density polyethylene tubing with one media type one-third the length of the other, but with inner and outer diameter dimensions identical. Each bioreactor was continuously operated with coarse bubble aeration and provided with a high ammonium loading to promote greatly active nitrifying communities. Biomass measurements were taken regularly to observe growth. A series of variable velocity gradient (G) batch tests was executed to determine the effect of mixing on mass transfer through the biofilms of each media type. High ammonium and variable pH

batch tests were also conducted to assess inhibition effects on nitrifiers. Greater biomass was consistently measured on the longer media despite both media types having similar ammonia uptake during continuous operation. Lower G values consistently produced greater ammonia utilization in the short media biofilm than in the long media biofilm. However, at mid to high range G values, ammonia consumption was similar between both biofilms. Ends of media typically had greater biomass and greater nitrate production than middle sections, while ammonia consumption was similar along carrier length. Abrupt changes in ammonium concentration and pH produced significantly greater inhibition effects in the short media biofilm than in the long media biofilm, suggesting greater protection in the biofilm grown on the longer media.

TABLE OF CONTENTS

LIST OF FIGURES

LIST OF TABLES

CHAPTER 1 INTRODUCTION

Problem Statement

Nutrient (N and P) removal is a critical function of wastewater treatment. Eutrophication is a result of excessive phosphorus and nitrogen discharge into natural water bodies from municipal wastewater systems. It is a leading cause in our nation's water degradation. The abundance of nitrogen and phosphorus stimulate algal bloom development which can lead to increased turbidity of natural waters, neurotoxin discharge from algae, as well as depleted dissolved oxygen content. In addition, ammonia is toxic to fish. All of these factors contribute to alterations, such as death of, the ecosystems initially present within the bodies of water and surrounding areas. Establishment of the Clean Water Act introduced the National Pollutant Discharge Elimination System (NPDES) to regulate point source discharge of nutrients, such as phosphorus and nitrogen, into surface waters.

Wastewater Treatment

Typically referred to as secondary wastewater treatment, biological removal of contaminants in wastewater is performed by suspended growth systems, such as activated sludge, or by biofilm-based technologies.

Activated sludge systems are the most common practice used in biological nutrient removal processes in industrialized countries. Consisting of a series of anoxic and aerobic tanks followed by a large settling basin (secondary clarifier), activated sludge systems utilized the growth of suspended flocs of biomass for degradation and removal of nutrients (Tchobanoglous et al., 2003). A recycle line from the secondary clarifier to

the series of anoxic tanks is incorporated into these systems to ensure a long solids

residence time (SRT) (Tchobanoglous et al., 2003). See Figure 1 for an illustration of this

system.
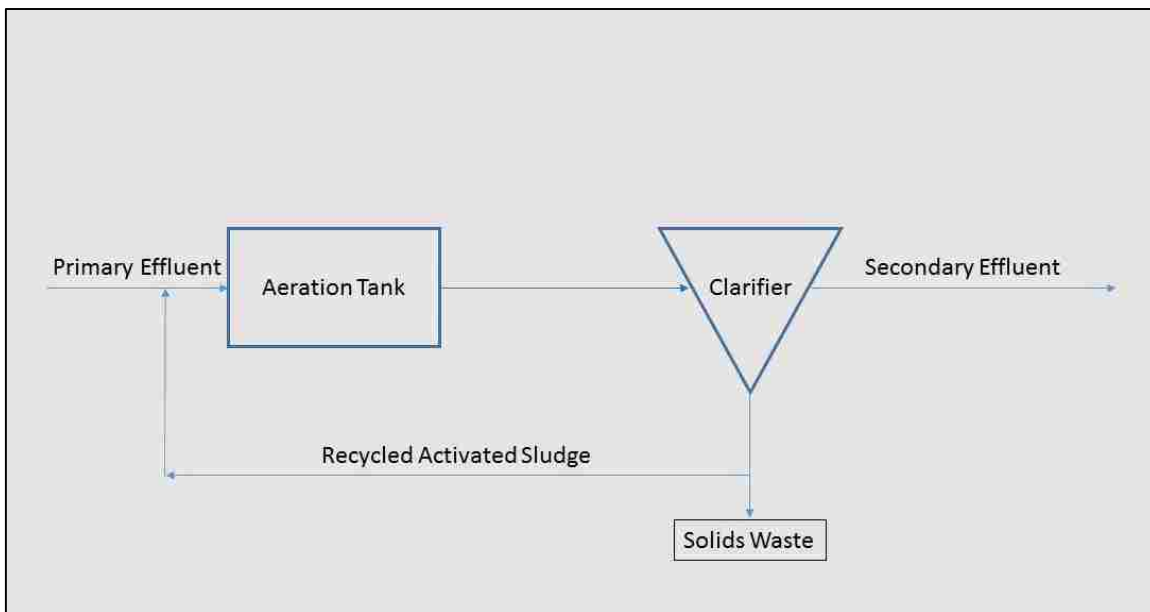
Figure 1 – Typical activated sludge system process with activated sludge recycle line.

Biofilm based systems require a growth surface for attachment and development. These

growth media can be fixed-in-place, as in trickling filters and packed bed reactors, or

they can be grown on mobile, free-floating media that mix with the reactor liquid

volume, as in moving bed biofilm reactors (MBBRs) and integrated fixed film activated

sludge (IFAS) systems (Ødegaard et al., 2006). MBBR and IFAS systems typically contain

plastic media with a high surface area favoring microorganism attachment and growth;

the result of biomass attachment to media is a much longer SRT than conventional

activated sludge systems (Rusten et al., 1995). Biofilm growth is particularly useful for

enrichment of nitrifying bacteria, which are slow growing autotrophs (Okabe et al.,

1999). Mass transfer in biofilm systems is dependent on: (1) diffusion across the mass transfer boundary layer and (2) diffusion into the biofilm driven by the concentration gradient in existence between the bulk solution and the substrate-depleted biofilm (Eberl et al., 2006, Henze et al., 2008). Figure 2 illustrates a simple MBBR process.
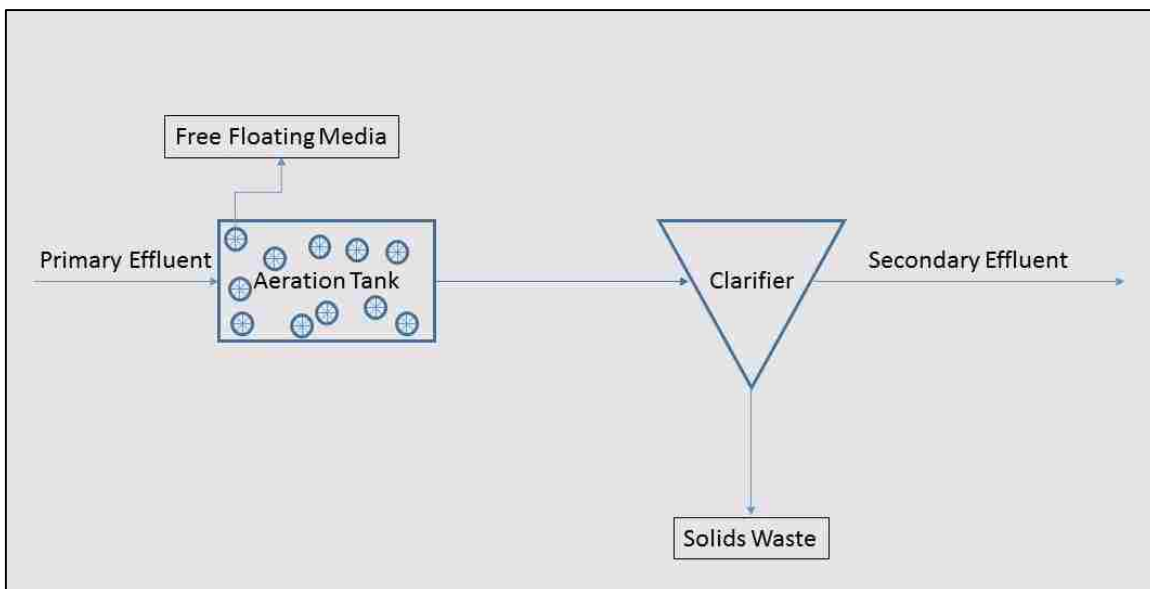
Figure 2 – The MBBR process does not require an activated sludge recycle due to the production and retention of biofilm on free-floating media.

Research Objectives

To our knowledge, there are no published studies of media morphology effects on nitrification, or wastewater treatment in general, where geometric sizes of attachment media have been systematically varied. It was expected that media with relatively more protected interiors tends to have relatively lower internal flow velocities, and it was hypothesized that this will have several measureable effects. It was hypothesized that:

(1) Media with a relatively more protected interior would result in greater amounts of biofilm due to less shearing of the biofilm surface.

(2) Media with relatively less protected interior has greater activity, due to greater advective flow through the media and an increase in the "edge effect" suggested by Bjornberg et al. 2009.

(3) The relationship between mixing rates and biofilm activity is dependent on media geometry, with a more protected interior being more sensitive to mixing than a less protected interior. This is due to a generally thicker laminar boundary layer in the more protected media with greater potential to be reduced by mixing than the thinner boundary layer in less protected media.

(4) Inhibition of AOB and NOB activity can be induced by increasing the inhibiting species concentration with increased loading rates or by pH speciation of that compound, but that a thicker biofilm grown in a more protected medium would be more resistant to inhibition.

The objective of this study was to test these hypotheses with a systematic variation of media geometry. The experimental approach was to operate laboratory scale MBBRs containing media of variable length, with a focus on nitrification activity and inhibition of said activity. A series of bench scale batch tests was also executed to assess the effect of mixing on nitrification. A comparison of edge and inner interior biofilm activity was

also performed. A series of bench scale batch tests was also performed with shock

loadings and pH changes to measure inhibition effects.

CHAPTER 2 BACKGROUND AND LITERATURE REVIEW

Nitrification in Nutrient Removal

Nitrification (ammonia oxidation) is a critical process in wastewater treatment systems.

IFAS and MBBR systems are commonly used to increase rates of nitrification, as the slow

growing autotrophic nitrifying bacteria are enriched in biofilms, at least in part because

of the relatively long residence times inherent to biofilm growth.

Nitrification occurs in two steps: ammonia oxidation to nitrite (nitritation) by ammonia

oxidizing bacteria (AOBs) and nitrite oxidation to nitrate (nitratation) by nitrite oxidizing

bacteria (NOBs). Both steps in nitrification are shown in Reactions 1 and 2.

AOBs oxidize ammonium to nitrite with production of hydronium ion as a separate

product which results in pH reduction during secondary treatment:

$$2NH_4^+ + 3O_2 \rightarrow 2NO_2^- + 4H^+ + 2H_2O \tag{1}$$

NOBs oxidize nitrite to nitrate:

$$2NO_2^- + O_2 \rightarrow 2NO_3^- \tag{2}$$

The total combined reaction is as follows (Reaction 3):

$$NH_4^+ + 2O_2 \rightarrow NO_3^- + 2H^+ + H_2O \tag{3}$$
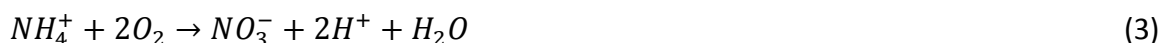
These bacteria use inorganic reduced carbon as their primary source for development and are classified as chemoautotrophs (utilize inorganic carbon) and therefore are also chemolithotrophic (utilize inorganic substrates) microorganisms. The nitritation step can be inhibited by high concentrations of FNA via increased loading rate or a drop in pH while the nitratation step is inhibited by increased FA loading rates or a rise in pH.

MBBR History

From 1972 to 2008, activated sludge system implementation has increased 27% while biofilm treatment expansion has remained stationary (Parker et al., 2010). In the late 1980s the MBBR process was patented (European Patent no. 0,575,314, US Patent no. 5,458,779) in Norway by Kaldness Miljoteknologi through its affiliation with the Foundation for Scientific and Industrial Research at the Norwegian University for Science and Technology (Ødegaard et al., 1994; Rusten et al., 1998). By the late 1990s, when MBBR and IFAS systems were available for nutrient removal applications, so many activated sludge systems were already installed in wastewater treatment plants an attractive option for integrating the MBBR process into an already existing secondary treatment process was by means of upgrading and retrofitting activated sludge systems as IFAS systems (Parker et al., 2010).

MBBR Retrofit to Municipal Wastewater Treatment

To achieve a greater efficiency in performance, or greater contaminant removal from wastewater, it is possible for activated sludge systems to be upgraded and retrofitted to

an MBBR or IFAS type system. This upgrade will require a shorter hydraulic residence time (HRT) to attain the same removal efficiency, which can be accomplished with a smaller volume aeration tank system, or will result in greater removal if the system HRT is unchanged; this is due to the greater capacity of the attached biofilm over suspended biomass to degrade nutrients (Javid et al., 2013). Biofilm attachment to media translates to a long SRT and makes biomass retention independent of biomass selection from secondary clarifiers (McQuarrey et al., 2011).

MBBR Media Design Effects

IFAS and MBBR media are commercially available in a variety of shapes and sizes, but there are few published studies of how media geometry affects biofilm development and performance. Ødegaard et al. 2006 reported that differences in carrier shape had no significant effect in performance despite the influence of shape on effective area for biofilm attachment. Bjornberg et al. 2009 examined MBBR media cross sections and determined that biomass attachment is more concentrated toward the edges of the media rather than the interior. These researchers suggested that interior biofilms are relatively inactive, and therefore media design with minimal interior area may have greater overall activity. Melcer and Schuler (2014) reported that varying mixing rates had a greater effect on a more protected MBBR media design than on MBBR media with a less protected interior, but geometric variables were not studied in a systematic way..

Nitrifier Inhibition in MBBRs

There are also few published studies of how media geometry affects biofilm resistance to inhibition. Park et al., 2009 demonstrated that ammonia oxidizing bacteria (AOB) and nitrite oxidizing bacteria (NOB) are inhibited by free nitrous acid (FNA) and free ammonia (FA) respectively (Anthonisen et al., 1976). Several studies have demonstrated FA inhibition of the nitratation step to encourage shortcut biological nitrogen removal via nitrite accumulation (Chung et al., 2007; Hellinga et al., 1998; Park et al., 2010).

MBBR Media Differences

Example MBBR media geometries are shown in Figure 3. This figure demonstrates the significant variability in media design geometry as well as effective surface area. Performance comparison between the same shape media or same effective surface area media is entirely absent.
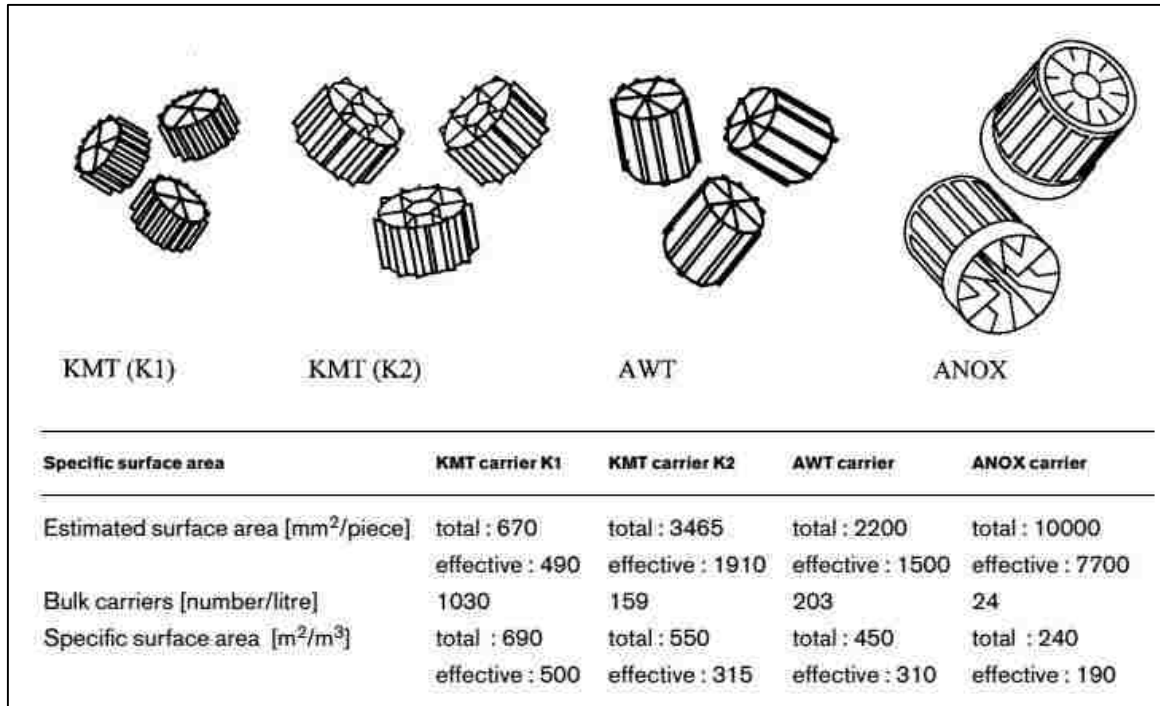
Figure 3 – Various media types used in MBBR and IFAS systems (Ødegaard et al., 2000).

Biofilm Mass Transport

Mass transport of a substrate in biofilm systems is often modeled with diffusion through an external laminar boundary lay of liquid, and diffusion and substrate uptake within the biofilm (Figure 4). Substrate transport through the mass transfer boundary layer (MTBL) described by Fick's First Law (Equation 1). Mass transport of substrates through the biofilm layer is dependent on Fick's First Law and Monod kinetics shown in Equations 1 and 2. (Tchobanoglous et al., 2003).

$$r_{MTBL} = -D\frac{dC}{dx} = -D\frac{(C_{bulk}-C_{biofilm})}{T} \qquad (1)$$

r_{MTBL} = rate of substrate flux across the MTBL (g/m^2•d)

D = diffusion coefficient of substrate in water (m^2/d)

dC/dx = substrate concentration gradient (g/m^3•m)

C_{bulk} = bulk liquid substrate concentration (g/m^3)

$C_{biofilm}$ = substrate concentration at the biofilm-MTBL border (g/m^3)

T = thickness of MTBL (m)

The rate of substrate utilization in the biofilm is dependent on the substrate

concentration at a point in the biofilm according to Monod kinetics:

$$r_{su} = -\frac{kSX}{K_S + S} \tag{2}$$

r_{su} = rate of substrate utilization in biofilm (g/m^2•d)

k = maximum specific substrate utilization rate (g/g•d))

S = substrate concentration at a point in the biofilm (g/m^3)

X = biomass concentration (g/m^3)

K_s = half velocity constant (g/m^3)
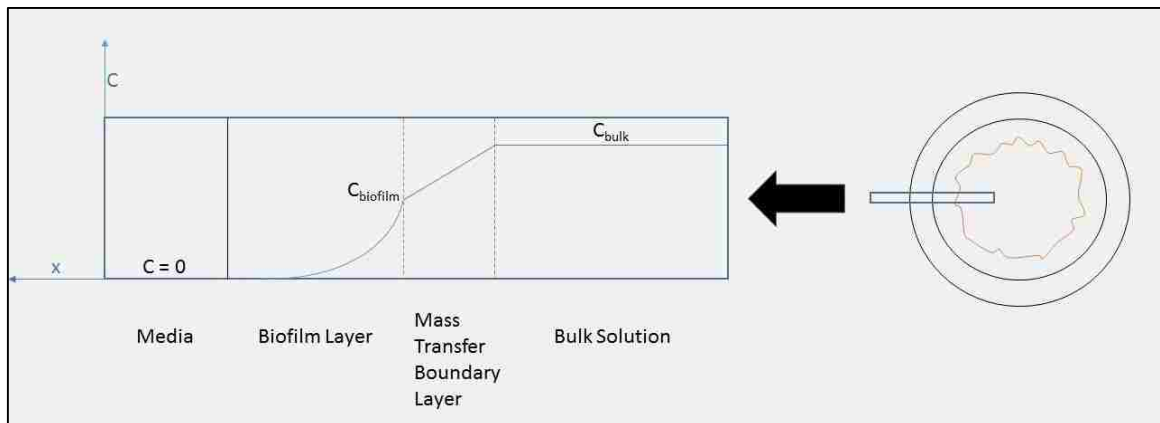
Figure 4 – Illustration representing substrate transport through the mass transfer boundary layer and into the biofilm according to Fick's First Law and Monod kinetics.

As substrates diffuse into the biofilm, the concentration gradient in between biofilm substrate concentration and bulk solution drives the substrate to the biofilm. Within the biofilm, both diffusion and substrate uptake occur. Biofilm substrate uptake rates will also vary within sections of the biofilm itself, as the biomass closer to the bulk solution is more active and therefore has a higher uptake rate than the biomass closer to the media where substrates and oxygen may be depleted (Boltz et al., McQuarrie et al., 2011).

CHAPTER 3 METHODS

Reactor Specifications

Two laboratory scale MBBR systems were constructed, one of which had shorter media

(R-Short) and one of which had longer media (R-Long). A reactor schematic is provided

in Figure 5, and key system parameters are provided in Table 1.
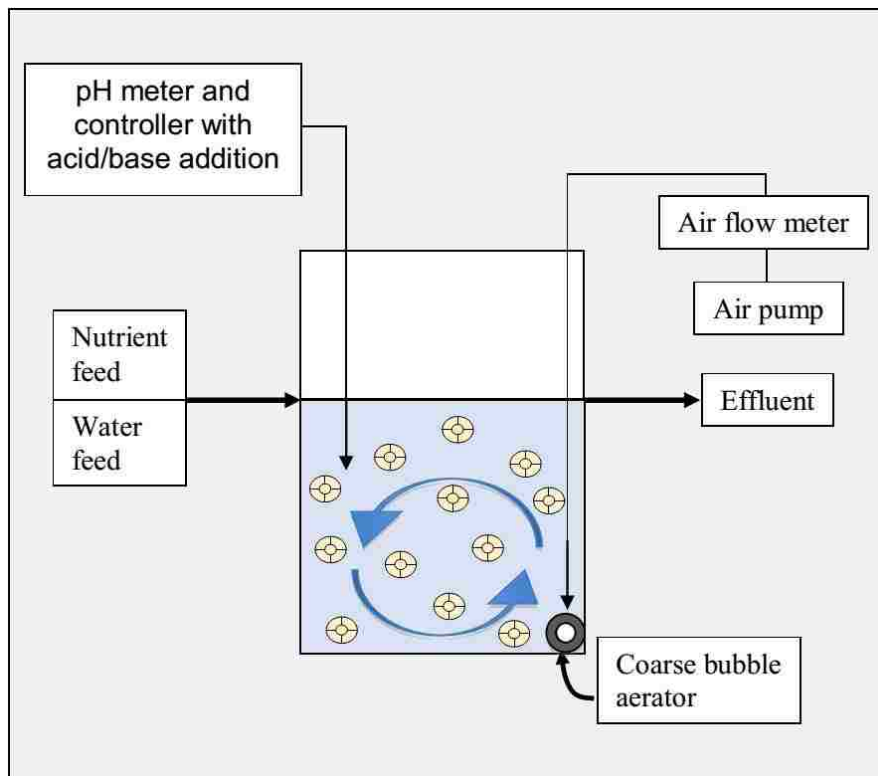
Figure 5 – Schematic for continuous flow MBBRs.

Table 1 –MBBR and media specifications.

Parameter	R-Short	R-Long
Working volume (liquid +media) (L)	10.5	10.5
Liquid volume (L)	9.56	9.56
Total influent flow rate (mL/min)	7	7
HRT (based on working volume) (h)	25.0	25.0
HRT (based on liquid volume) (h)	22.7	22.7
Media fill volume (%)	27	27
Inner diameter (mm)	4.76	4.76
Outer diameter (mm)	7.94	7.94
Media length (mm)	7.5	22.5
Number of media in reactor	4064	1355
Total biologically active internal surface area (m^2)	0.46	0.46
Specific biologically active surface area (m^2/m^3)	43.4	43.4

Media

In order to study the effect of media length on biofilm growth and activity, custom

media was made by cutting high-density polyethylene (HDPE) tubing into 7.5 mm (R-

Short) and 22.5 mm (R-Long) sections (Figure 6 and Table 2). Each reactor contained 100

feet total of media, resulting in a fill volume (volume of media, including voids, divided

by the total reactor volume) of 27 %. It is common practice to report the internal surface

area as the biologically active area in MBBR systems, as the external surfaces are

scoured by collisions with other media (Figure 7). The specific biologically active surface

area in each reactor was 43.4 m^2/m^3. The total surface area of 0.46 m^2 is the area used

in all calculations of substrate flux.
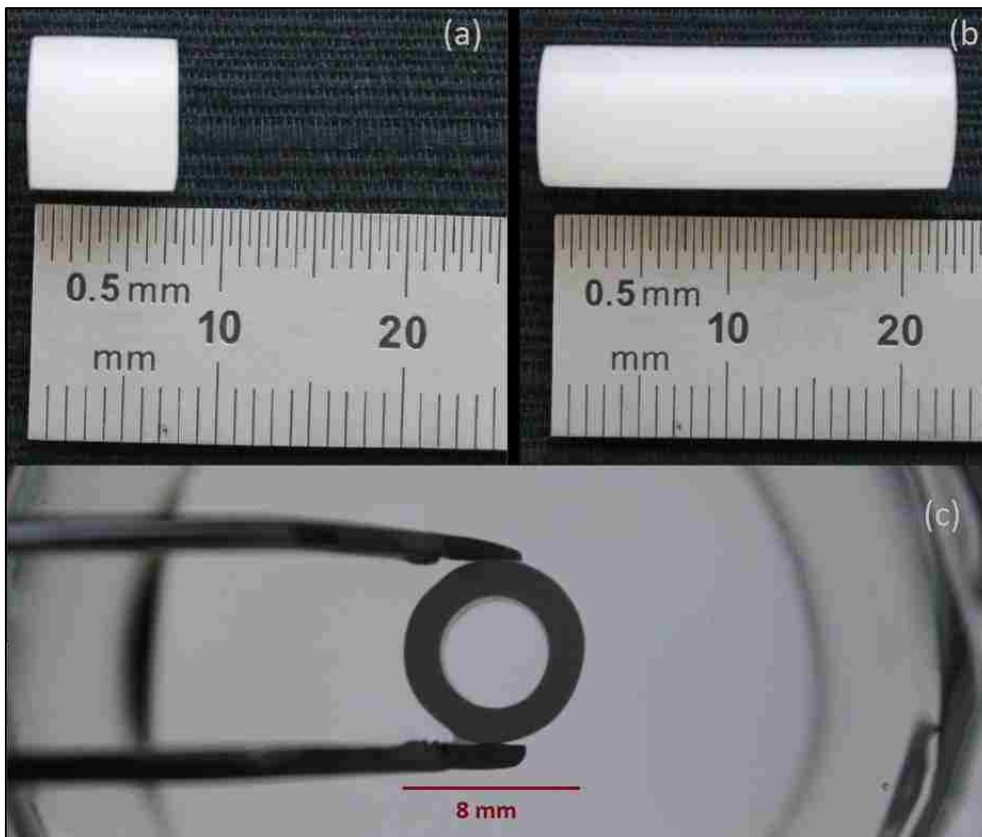
Figure 6 – (a) R-Short media; (b) R-Long media; (c) Media cross section
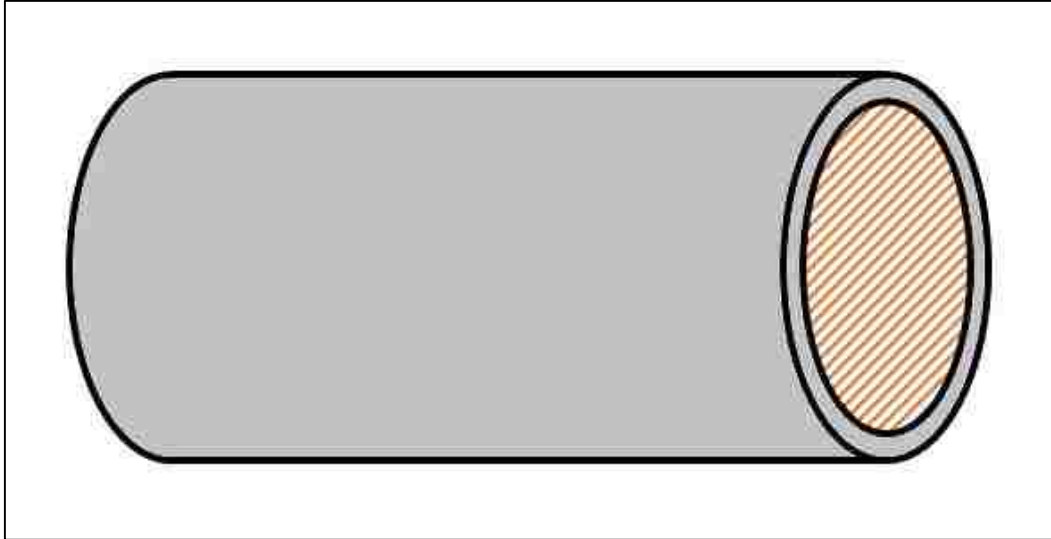
Figure 7 – An example carrier is shown with the biologically active area (effective area) as the striped surface.

Synthetic Feed

The synthetic feed was added as a concentrated stream (2.2 mL/min) diluted with dechlorinated tapwater (4.8 mL/min) to reduce the volume of feed requiring preparation. The net (diluted) feed concentrations are shown in Table 2. Influent ammonia concentrations were gradually increased during the startup phase, with a goal of maintaining effluent concentrations in the range 10 to 30 mg NH_4-N/L. This was intended to avoid ammonia limitation of nitrification activity and also ammonia inhibition of NOBs (Kim et al., 2005). Upon startup, the influent ammonia concentrations were maintained at 20.5 mg NH_4-N/L until the reactors reached a maximum of 200 mg NH_4-N/L. These ammonia concentrations were high relative to domestic wastewater to produce highly nitrifying biofilms, and no reduced carbon was

included to reduce competition for space from heterotrophs. Synthetic feed was

prepared with autoclaved glassware to ensure sterile conditions.

Table 2 - Synthetic Feed (based on Hem et al., 1994)	
Chemical	**Concentration (mg/L)[a]**
NH_4Cl	Variable (see text)
KH_2PO_4	100
$NaHCO_3$	350
$FeSO_4\text{-}7H_2O$	5
$CaCl_2$	16
$MgSO_4\text{-}7H_2O$	40
$CuSO_4\text{-}5H_2O$	0.12
$NaMoO_4$	0.0019
EDTA	6.6

MBBR Construction and Assembly

Prior to MBBR startup, the following components of the laboratory scale MBBR design

were acquired:

(1) Reactor Bodies

Two acrylic plexiglass rectangular prisms with one open end were constructed by Desert

Plastics. The base of each reactor body was 8.375" X 8.375" with a height of 17". At

10.5" from the base of the reactor a 0.25" NPT fitting was integrated into the design for

quick connecting and disconnecting of the effluent line (Figure 8)
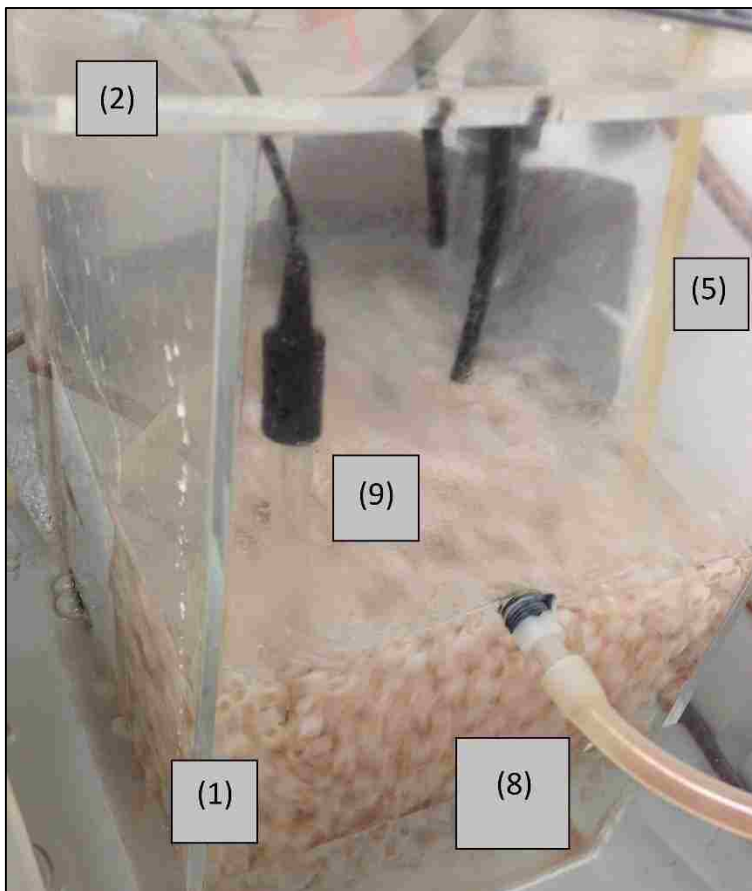
Figure 8 – MBBR body.

(2) Reactor Lid

A 10.5" X 10.5" reactor lid was constructed with five holes with the following specifications for diameter: acid line (3/8"), base line (3/8"), pH electrode (3/4"), air line (1/2"), and nutrient feed (3/8") (Figure 9).
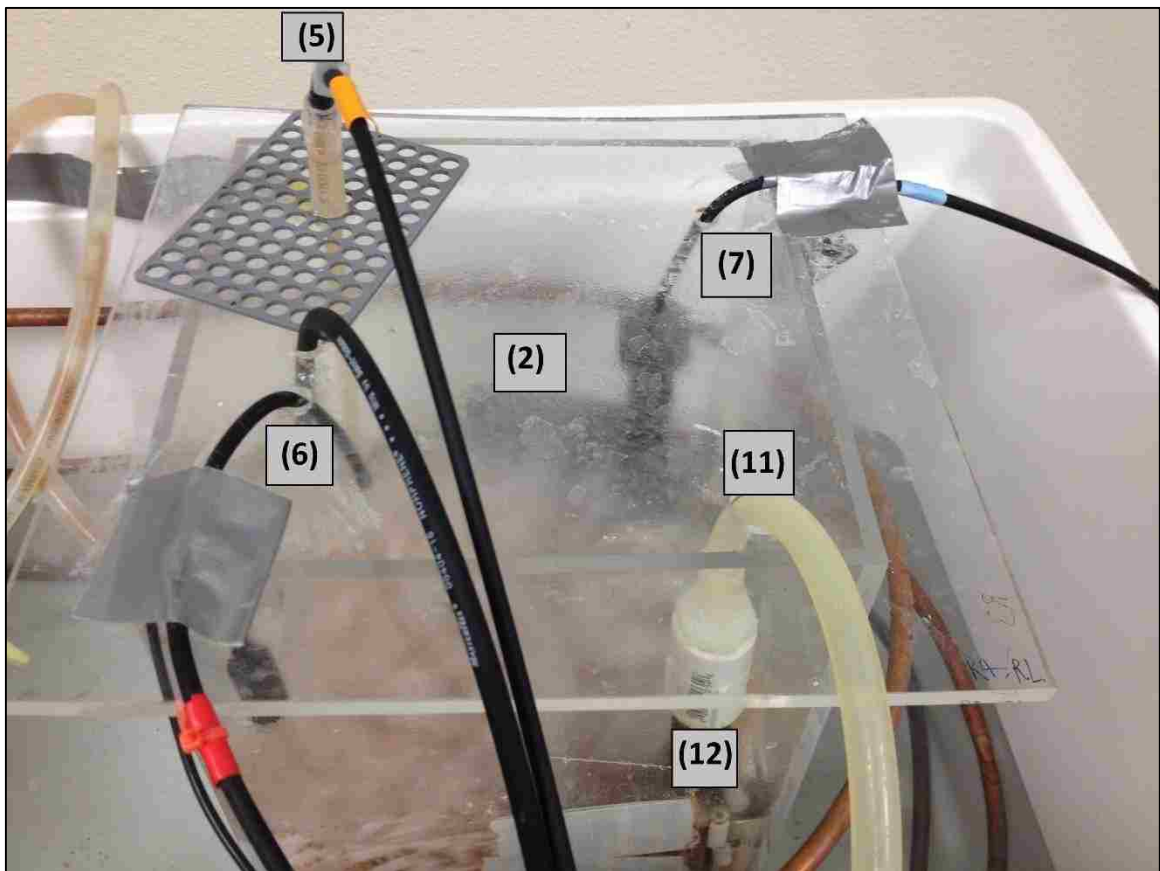
Figure 9 - MBBR lid and components.

(3) Nutrient Feed Pump Configuration

A Cole-Parmer Masterflex L/S Standard Drive Peristaltic Pump 7523-10 was used for each reactor's nutrient feed. The pump heads used were Masterflex L/S Easy-Load Lab Peristaltic Pump HEAD,Cole-Parmer 7518-00 with Masterflex Norprene tubing (A60 G), L/S 14 (Figure 10).

(4) Water Feed Pump Configuration

A Cole-Parmer Masterflex L/S Standard Drive Peristaltic Pump 7520-10 (3224) was used for each reactor's water feed. The pump heads used were Masterflex L/S Easy-Load Lab Peristaltic Pump HEAD,Cole-Parmer 7518-00 with Masterflex Norprene tubing (A60 G), L/S 14 (Figure 10).
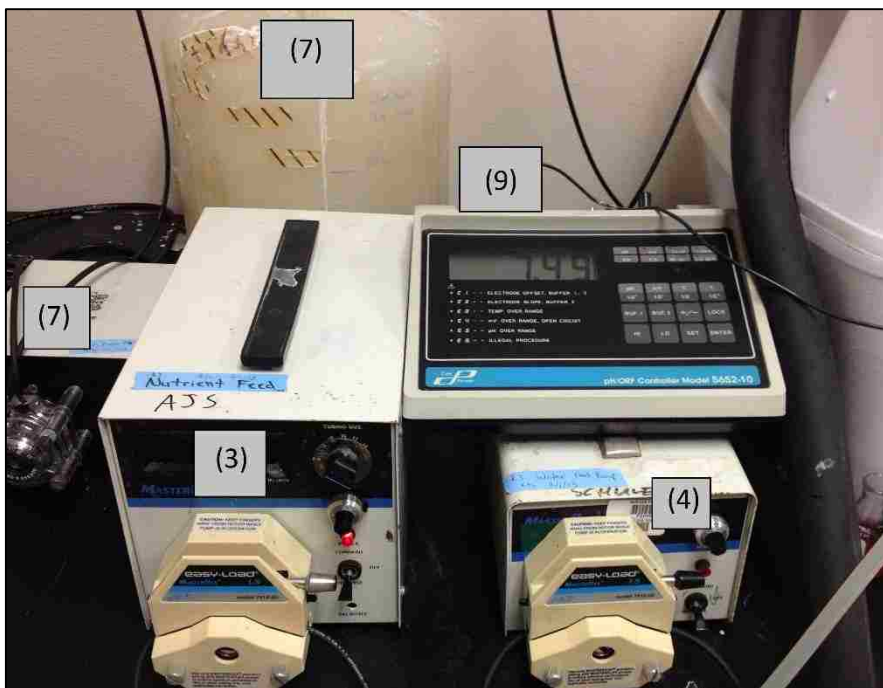
Figure 10 – Water, nutrient, base, and pH setup.

(5) Influent Configuration

The water feed (4.8 mL/min) and nutrient feed (2.2 mL/min) were combined in a
separate line before entering the reactor at 7 mL/min (Figure 9).

(6) Acid Pump Configuration

A Cole-Parmer Masterflex 7543-30 Pump was used for each reactor's acid line. A
Masterflex 7014-52 pump head was used for each pump with Masterflex Norprene
tubing (A60 G), L/S 14 (Figure 11).

(7) Base Pump Configuration

A Cole-Parmer Masterflex 7540-30 Pump was used for each reactor's base line. A
Masterflex 7014-52 pump head was used for each pump with Masterflex Norprene
tubing (A60 G), L/S 14 (Figure 10).

(8) Effluent Line Configuration

A Cole-Parmer Masterflex 7543-30 Pump was used for each reactor's effluent line. A
Masterflex 7014-52 pump head was used for each pump with Masterflex Norprene Food
tubing (A60 F), L/S 17 (Figure 11).
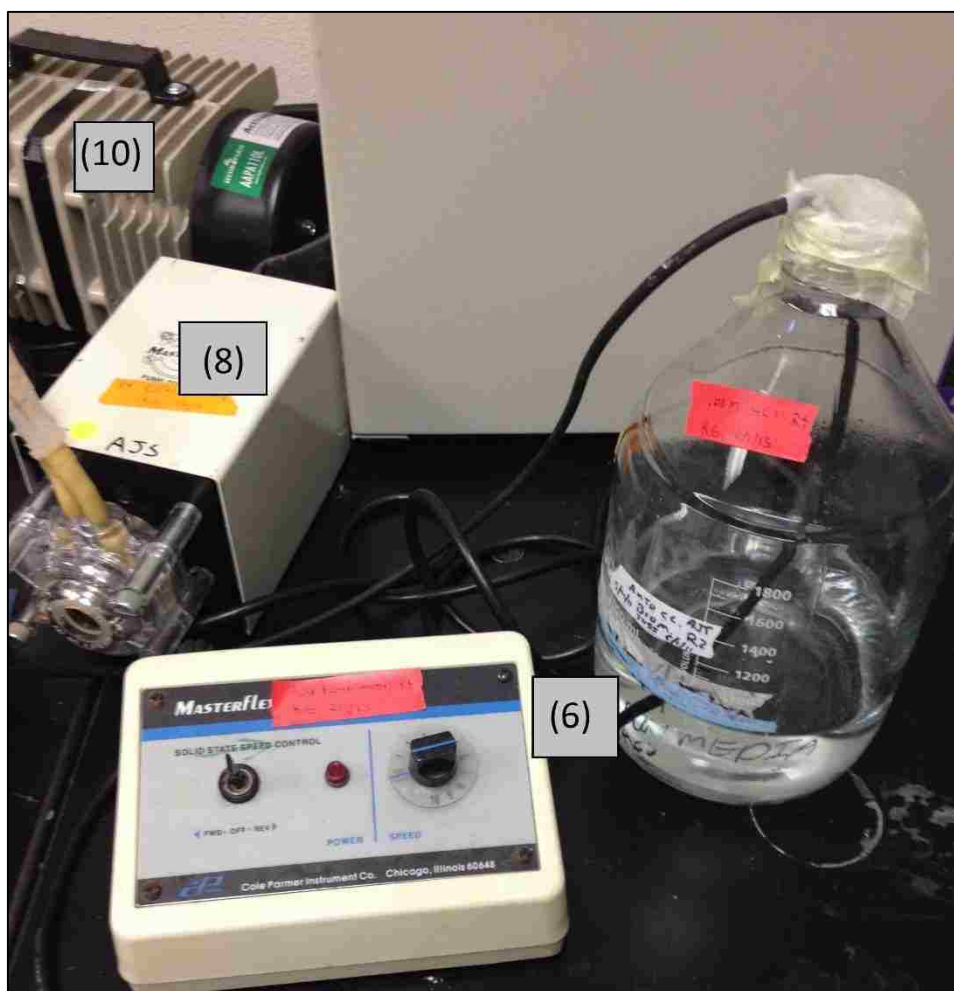
Figure 11 – MBBR acid, effluent, and air setup.

(9) pH Control Configuration

Acid and base pumps were connected to, and controlled, with a Cole Parmer pH/ORP

Meter/Controller 5652-10. A Cole-Parmer combination, double-junction, gel filled, pH

electrode was connected to the pH meter (Figure 10).

(10) Air Pump Configuration

A Hydrofarm AAPA110L 112-Watt 110-LPM Active Aqua Commercial Air Pump was used for each reactor's coarse air bubble mixing. Dow Corning Pharma-50 Tubing, 1/4" x 7/16" was used for directed air flow (Figure 12).

(11) Air Flow Control

A RMC-106-BV, 10-100 SCFH Flowmeter was used in conjunction with Dow Corning Pharma-50 Tubing, 1/4" x 7/16" was used for directed air flow into the reactor (Figure 12).
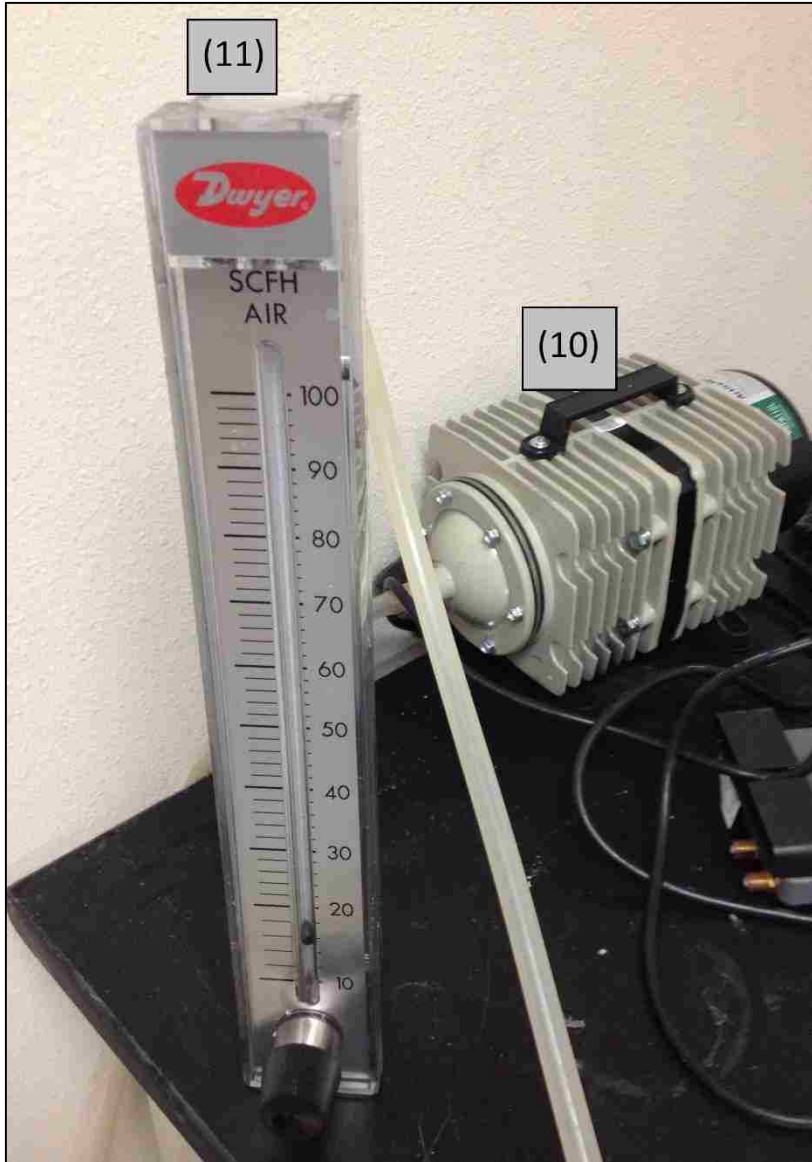
Figure 12 – Air flow and control for coarse bubble mixing.

(12) Aerator

The aerator was constructed with three 1/2" X 6" PVC Nipple Fittings, Double Threaded,

and a 1/2" NPT Male X 1/4" Barbed, Polypropylene Hose Fitting, Adapter (Figure 9).

(13) Water Feed Container

The water feed was stored in 50L Nalgene, HDPE, Carboys (Figure 13).

(14) Nutrient Feed Container

The nutrient feed was stored in a 20L Pyrex, Autoclavable, Carboy (Figure 13).

Figure 13 – Water and nutrient feed storage.

(15) Water Bath Configuration

Each MBBR was assembled and placed into a Rubbermaid 150 Qt. Gott™ Marine Cooler which was filled halfway with tap water and surrounded by copper coiling. The coiling was connected to Pharma-50 Tubing, 1/4" x 7/16" which was connected to a Cole-Parmer Polystat Standard 6L Heat/Cool Bath, -20 to 100 °C; 115VAC. This provided a strict temperature control in each reactor (Figure 14.)
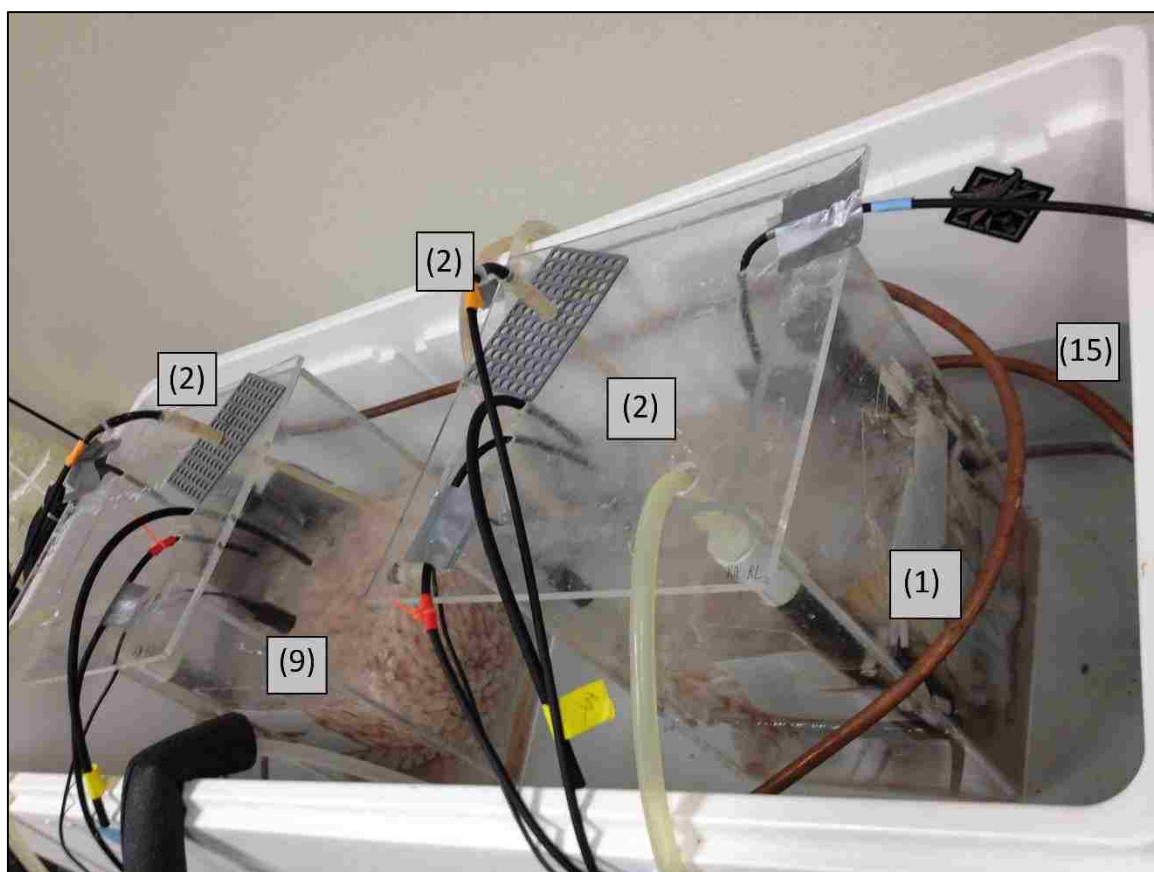
Figure 14 – R-Short (left) and R-Long (right) contained in the water bath.

Reactor Operation

Before startup, both carrier types were separately inoculated in 10 L of fresh activated

sludge from the Albuquerque, New Mexico, Southside Wastewater Reclamation Plant

(SWRP) for 3 days at room temperature with coarse-bubble mixing. The SWRP uses a

Modified Ludzack-Ettinger configuration. After 3 days of inoculation, the media solution

in each MBBR was replaced with 5 L of settled activated sludge and 5 L of fresh primary

effluent. The continuous synthetic feed was then introduced to each reactor.

The pH of each reactor was kept between 7.15 and 7.50 using a pH controller with 0.5 M

HCl and 0.7 M $NaCO_3$. The temperature was 21 degrees Celcius (°C). The reactors were

brushed daily to prevent biofilm growth on the walls. Each reactor used a coarse bubble

aerator and a velocity gradient (G) value of 291 s^{-1} was maintained by course bubble

aeration at a flow rate of 42 scfh, calculated with Equation 3 (Tchobanoglous et al.,

2003). The G value of 291 s^{-1} was based on the full scale system range of 134-360 s^{-1}

reported by Melcer and Schuler (2014). The values of G used in batch testing are

summarized in Table 3.

$$G = \sqrt{\frac{P}{\mu V}} \Rightarrow G = \sqrt{\frac{Q*\gamma*H_L}{\mu V}} \qquad (3)$$

G = velocity gradient (1/s)

P = pump power (J/s)

Q = airflow rate (m^3/s)

γ = water specific weight (N/m^3)

H_L = head loss (m) (distance from aerators to water surface)

μ = water dynamic viscosity ($N*s/m^2$)

V= volume (m^3) (working volume)

* Equation 3 assumes a pump efficiency of 100%

Table 3 - G Values and Corresponding Air Flow Rates	
G (1/s)	Q (scfh)
185	17
211	22
254	32
291*	42
342	58
362	65
381	72

A * G value of 291/s was used during continuous operation.

Batch Tests

Variable G batch tests were performed on the media cultured in the continuous systems to evaluate the effects of mixing on activity with different media geometries. These tests were performed in the continuous system reactors with the influent and effluent pumps stopped. Batch tests were performed only after each system reached a state of equilibrium. One to six batch tests were performed in one day and batch testing days were at least 2 days apart.

The batch test solution was the same as the reactor net feed (Table 2), with the

ammonia concentration equal to approximately 30 mg NH_4-N/L. The media were gently

removed from the reactors and the liquid volume was removed separately. The media

were gently rinsed with fresh batch test solution, and the reactor was cleaned with DI

water, and rinsed with batch test solution. The media was replaced in each reactor and

filled with batch test solution to the original total volume (10.5 L). Mixing was

commenced via aeration to provide a target G value, which was varied across a series of

batch tests on a given day, and a 5 mL sample was quickly taken and filtered through at

0.45 μm filter to mark t=0. pH was controlled at 7.25 ±0.05 during the batch tests.

Additional samples were taken up to one hour.

Additional batch tests were performed to evaluate potential differences in activity of

biofilm grown in the center and the edges of the R-Long media. 13 media pieces were

taken from R-Long and cut into 3 equal sections with a pipe cutter. 13 end sections and

13 middle sections were tested separately in 100 mL batch tests, providing

approximately the same specific surface area as in the continuous systems (the

remaining 13 end pieces were discarded). 13 media from R-Short were also tested in a

100 mL batch reactor for comparison. After cutting, media pieces were gently rinsed

with batch test solution. Two sets of tests were performed. In the first, the batch test

solution was as in Table 2 but with 40 mg NO_2^--N/L and 0 mg NH_4-N/L added to observe

nitratation (NOB activity) only. The second batch test included 40 mg NH_4-N/L and 40

mg NO_2^--N/L to observe AOB and NOB activity. pH was 7.35 at the beginning of the test,

and was measured but was not controlled. The media were added to the 100 mL

working volume batch reactors (150 mL Erlenmeyer flasks over Fisher Scientific Auto
Mixers) and mixing was provided via stir bar/plate at 100 rpm). At the start of the test a
0.5 mL sample was taken from each reactor and filtered through a 0.45 µm nylon filter
for nitrogen analyses as described below. Additional samples were taken and measured
during the test.

Analytical Methods

Nitrogen species were measured on 0.45 µm filtered samples using using Hach kits for
ammonia (AmVer TNT High Range Set), nitrite (NitriVer 3 TNT Low Range Set), and
nitrate (NitraVer X High Range Reagent Set) using a Hach DR-2700 spectrophotometer.
Samples were diluted as necessary to measure in recommended ranges.

Biofilm biomass was measured on randomly selected carriers (12 for R-Short and 4 for
R-Long, providing the same total surface area of each type). Biomass was removed from
the media by brushing using Proxabrush dental cleaning tools (GUM Between Teeth
Cleaning) and rinsing with DI water. The number of media removed from each reactor
was accounted for in continuous system calculations. The removed biomass was
measured using Standard Methods 2450B and 2540E (American Public Health
Association et al., 2012) for total suspended and volatile suspended solids, respectively,
and the reactor total biofilm solids (TBS) and volatile biofilm solids (VBS) were calculated
based on the total number of media in the reactors (Equation 4).

$$VBS = \frac{M_{550°C}}{V} \times \frac{T_{media}}{S_{media}} \qquad (4)$$

VBS = volatile suspended solids (mg/L)

$M_{550°C}$ = dry mass volatilized in 550°C oven (mg)

V = reactor working volume (L)

T_{media} = total number of media in reactor (#)

S_{media} = sample number of media used for biomass calculation (#)

CHAPTER 4 RESULTS AND DISCUSSION

Continuous Performance

During the startup phase of the study, the influent concentration to both reactors was gradually increased from 20.5 to 200 mg NH_4-N/L (Figure 15) to reduce potential ammonia inhibition by keeping reasonably low reactor (equal to the effluent) ammonia concentrations while also avoiding ammonia limitation for growth. The target effluent NH3 concentration was 10- to 50 mg N/L.0.

The two reactors demonstrated similar ammonia uptake (calculated as the influent – effluent ammonia concentrations) throughout the study (Figure 15). However, R-Long produced greater nitrate and lower nitrite concentrations than R-Short through much of the study (approximately days 50 to 100). R-Long also had greater ammonia uptake during instances of high effluent ammonia (days 50 to 100 for example) suggesting a

more active, or at least a more tolerant, AOB community than R-Short at higher effluent ammonia levels. After 105 days of continuous operation, each MBBR achieved a maximum ammonia uptake of approximately 180-190 mg NH_4-N/L. Influent ammonia concentrations were maintained at near 200 mg NH_4-N/L thereafter. Also after 105 days the ammonia uptake and nitrite and nitrate production reached steady states, and were nearly the same.
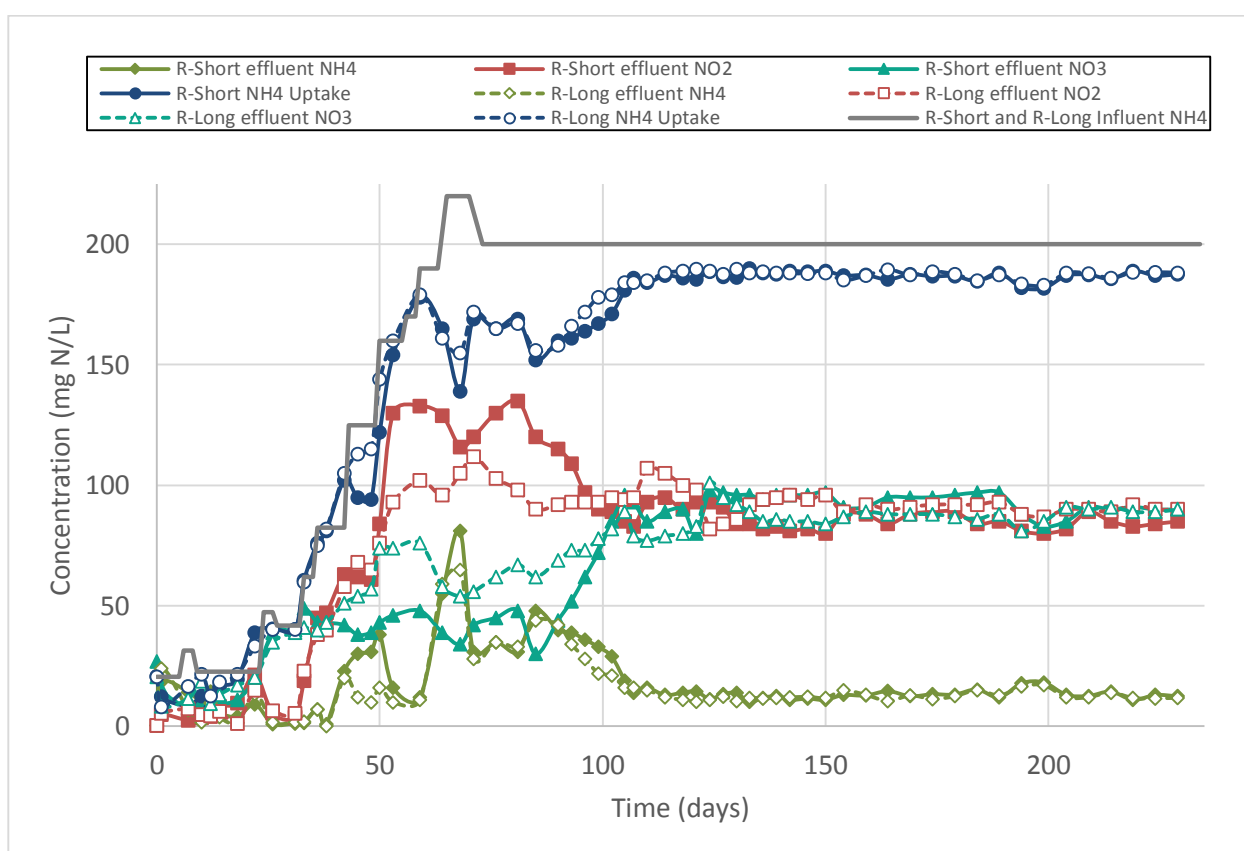
Figure 15 – Continuous operation; nitrogen species of interest.

Biofilm Growth and Attachment

Biofilm growth in the two reactors is shown in Figure 16. The R-Long media consistently had 78% higher biomass concentrations (approximately 0.41 mg VBS/cm^2 at steady state) than the R-short media (approximately 0.23 mg VBS/cm^2 at steady state), although the ammonia uptake from each reactor was similar (Figure 15). These results are consistent with media cross sections indicating a thicker biofilm in the R-Long media than in the R-Short media (Figure 17). In addition, the R-Long biofilm growth reached a steady state concentration more quickly (approximately 59 days) than did the short media (approximatetly 85 days; Figure 16). The R-Long media provided greater resistance to flow through the media than the R-Short media, leading to lower flow velocities and lower shear forces than in R-Short. The ammonia uptake was similar in both reactors after 105 days (Figure 15) despite differences in biofilm concentrations.
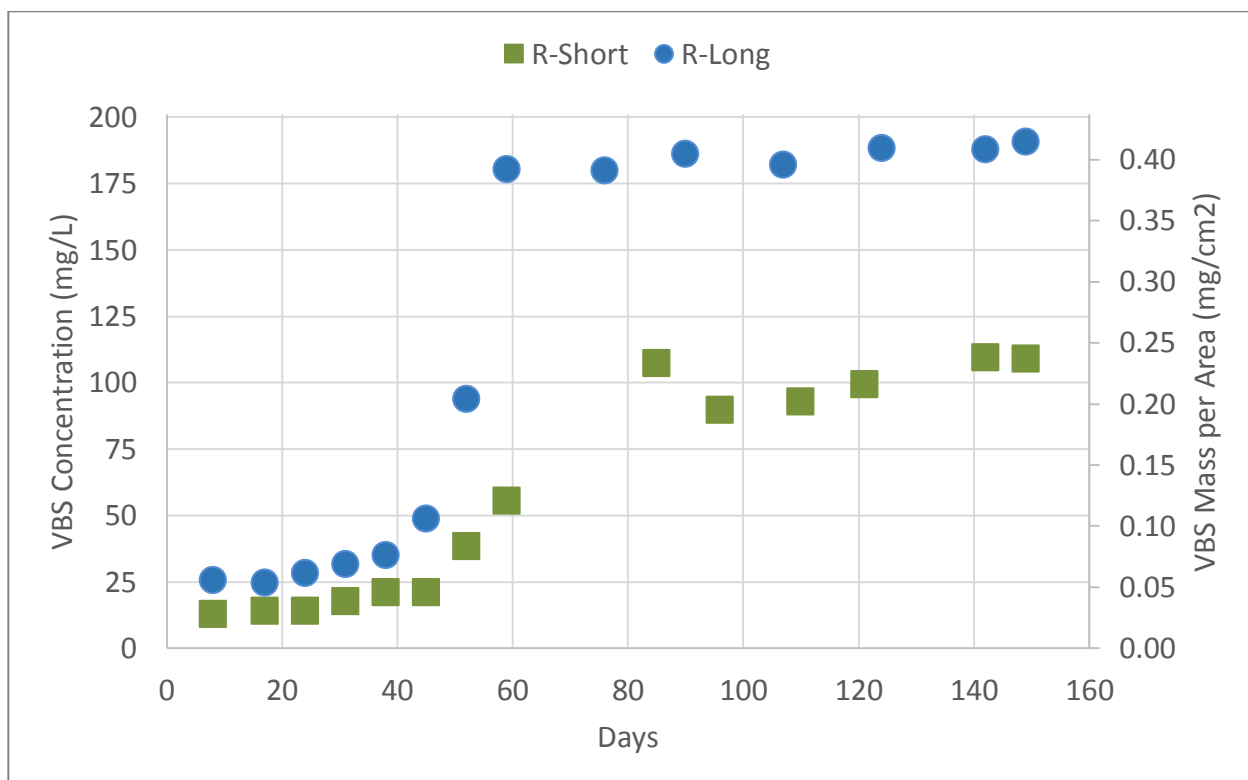
Figure 16 – Biomass measurements during MBBR operation.
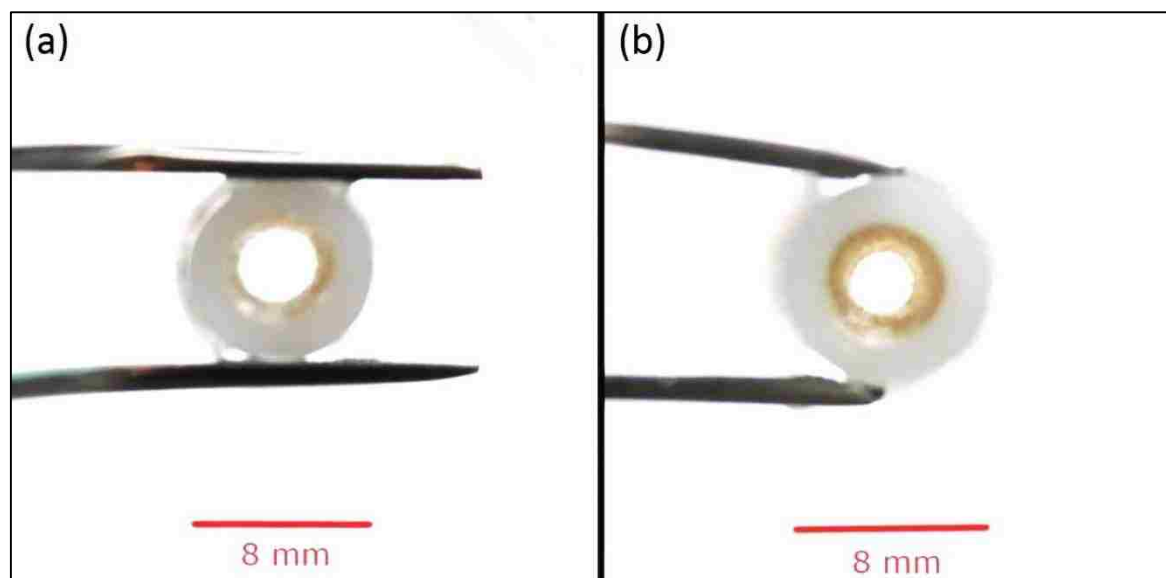
Figure 17 – Cross-sectional photos of media and biofilms at approximate steady state.

(a) R-Short ; (b) R-Long.

To ensure that activity was dominantly attributed to attached biomass rather than suspended biomass, total suspended solids (TSS) and volatile suspended solids (VSS) of the reactor fluid were measured. Table 4 shows the results of these measurements. Initially TSS and VSS concentrations were elevated, at 1910 mg/L and 1520 mg/L respectively, due to the startup reactor fluid content, primary effluent and activated sludge. After one week suspended fluid concentrations of VSS (and TSS) reached 10 mg/L. Hereafter, suspended fluid concentrations remained less than 1 mg/L while attached biomass measurements were significant. This suggests that AOB and NOB activity was coming from attached biomass and not suspended floc biomass.

Table 4 - TSS and VSS of Suspended Fluid		
Day	TSS (mg/L)	VSS (mg/L)
0	1910	1520
7	10	10
30	0.2	0.1
60	0.3	0.1

Variable G Batch Testing

The potential effects of media length on the relationship between mixing and biofilm activity were evaluated in batch tests of the two media types with variable mixing rates.

The minimum G value required for media mixing was determined to be 185 s^{-1} (at lower values dead zones of non-mixing media occurred), and so this was the minimum mixing value used in the batch tests. For both media, the relationship between mixing rates and ammonia flux (per biologically active, or internal, media area) followed an approximately saturation-type relationship. Melcer and Schuler, 2014, reported similar results, and modeled the relationship as half-order.

A typical batch test required measurements of ammonia, nitrite, and nitrate at 30 minute intervals. A typical batch test is shown in Figure 18.
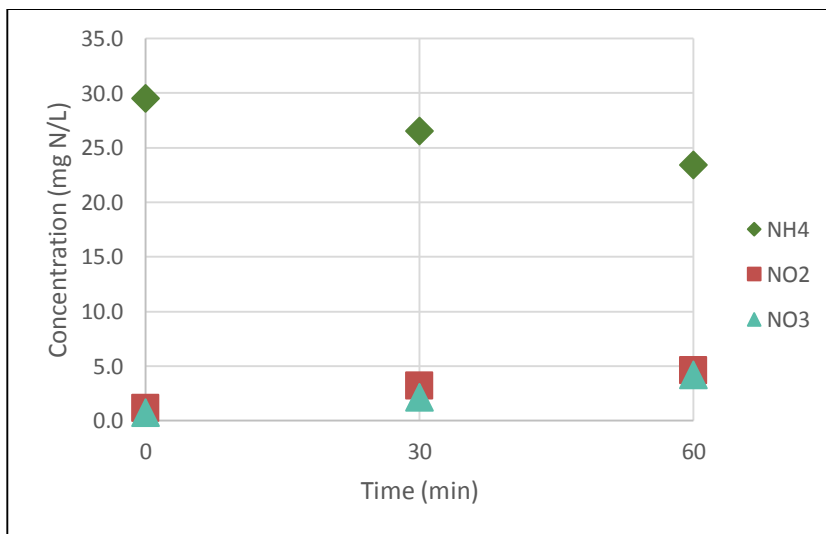
Figure 18 – Typical batch test conducted in R-Long at 21°C, pH = 7.25, DO = 6.75 mg/L, and G = 362/s. Ammonia utilization was fitted with a linear regression with R^2 = 0.99.

Ammonia flux rates were calculated from the measured concentrations using Equation

5. Ammonia concentrations were measured up to one hour and reactor volume was

constant. The effective surface area of media was calculated from number of media

present in the reactors.

$$J = \frac{dC}{dt} \times \frac{V}{A}$$
(5)

J = flux rate (g/(m^2•d))

dC = concentration differential (g/m^3)

dt = time differential (d)

V = working volume (m^3)

A = total active biofilm surface area (m^2)

Between mixing rate G values of 185/s and approximately 342/s, the R-Short media

resulted in higher nitrification rates (expressed as ammonia nitrogen flux) than the R-

Long media, while at 342/s and higher G values, the rates were similar (Figure 19). From

G = 185 to 254/s R-Short flux was approximately 0.45 g/(m^2•d) greater than that of R-

Long on average (Figure 19). At the higher G values, both media had similar ammonia

flux values of approximately 3.1 g/(m^2•d). It therefore appears that at high velocity

gradient (mixing) values, the media length had no effect on ammonia flux, while at

lower velocity gradient values shorter media yielded higher ammonia fluxes.

These results in Figure 19 demonstrated that the shorter media was less sensitive to mixing than was the longer media, with the shorter media flux having increased from 2.43 to 3.15 g/m^2•d as mixing was increased from 185 to 342 s^{-1}, while the longer media increased from 1.92 to 3.16 g/m^2•d over this range. Consequently, the R-Long media flux increase was 72% greater than the R-Short media flux increase from lowest to highest G (Figure 19 and Table 5). These results were consistent with the hypothesis that increasing media length results in a lower internal flow velocity, as noted above, and a thicker boundary layer. A thicker boundary layer provides greater resistance to mass transport into and out of the biofilm, and so increasing mixing has greater potential to increase mass transport with a thicker biofilm. In addition, it is possible that differences in the concentrations towards the middle of the media played a role in these results; for example, the lower internal flow velocity present in the longer media would result in lower ammonia and oxygen concentrations towards the middle of the media due to flux into the biofilm, which would tend to decrease rates of reaction toward the media middle, particularly at lower mixing rates when internal flow velocities are minimal. As mixing rates increase, the concentrations along the length of the media approach those of the bulk media. Because this effect is expected to be less pronounced in shorter media, it could also explain the observed differences in responses to mixing by the two media. The relative contribution of these two phenomena to observed differences between the two media is not known.

Nitrate production was also measured in R-Short and R-Long (Figure 20). Flux rates were very similar between R-Short and R-Long ranging from 0.98 to 1.50 g/m^2•d from lowest

to highest G values. However, this test was likely nitrite limited, the batch test starting nitrite concentration was 0 mg/ L NO_2^--N, and therefore prompted further NOB activity testing, the results of which are described in subsequent sections.

Melcer and Schuler, 2014, reported flux rates on the same order of magnitude to those in Figure 19, with one MBBR yielding a flux rate range of 1.2-2.4 $g/m^2 \bullet d$ and a second MBBR yielding the range of 1-4.2 $g/m^2 \bullet d$ for G values of 180 to 381 s^{-1}. These rates are comparable to R-Long and R-Short flux of 2.46 to 3.10 $g/m^2 \bullet d$ and 1.97 to 3.11 $g/m^2 \bullet d$ respectively over the same range of G values.

Melcer and Schuler, 2014, also reported media coefficient values (k), based on their half order empirical model for ammonia flux, for both media types which are on the same order of magnitude as the k values for R-Short and R-Long media (Table 5). Despite these lower k values, R-Short and R-Long achieved similar flux rates to the Melcer and Schuler, 2014 study.
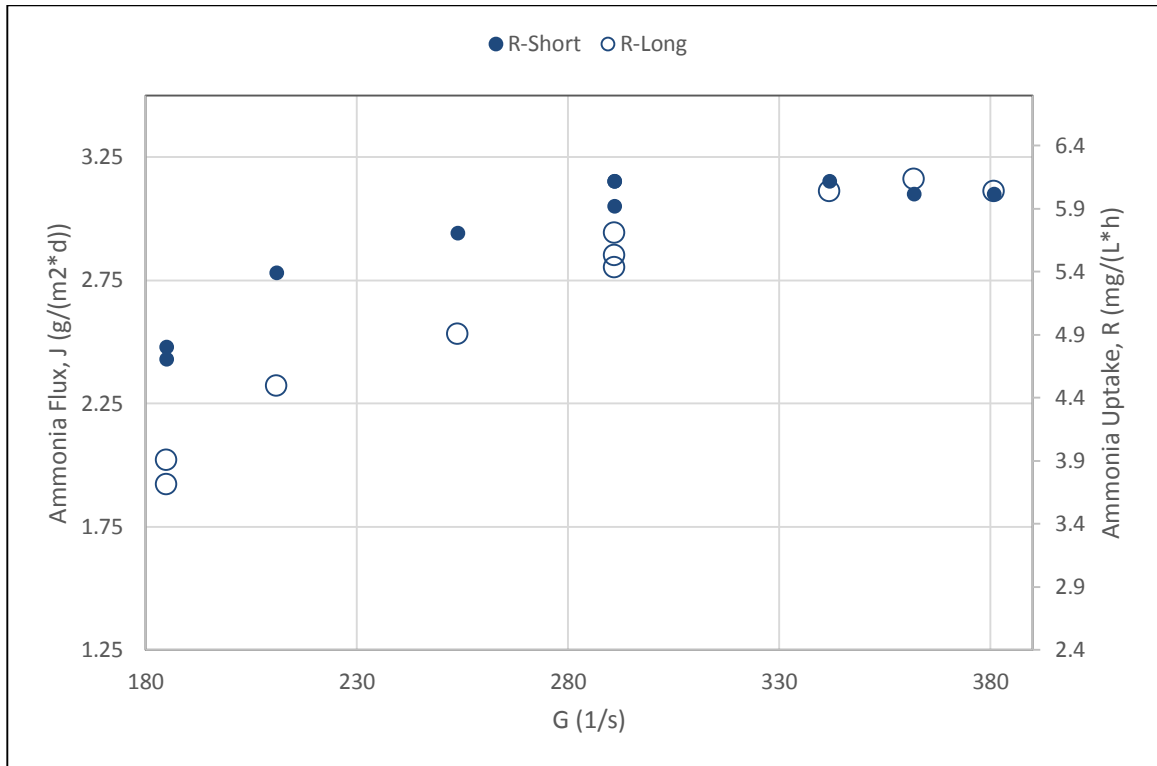
Figure 19 – Batch test ammonia utilization by R-Short and R-Long (AOB Activity).
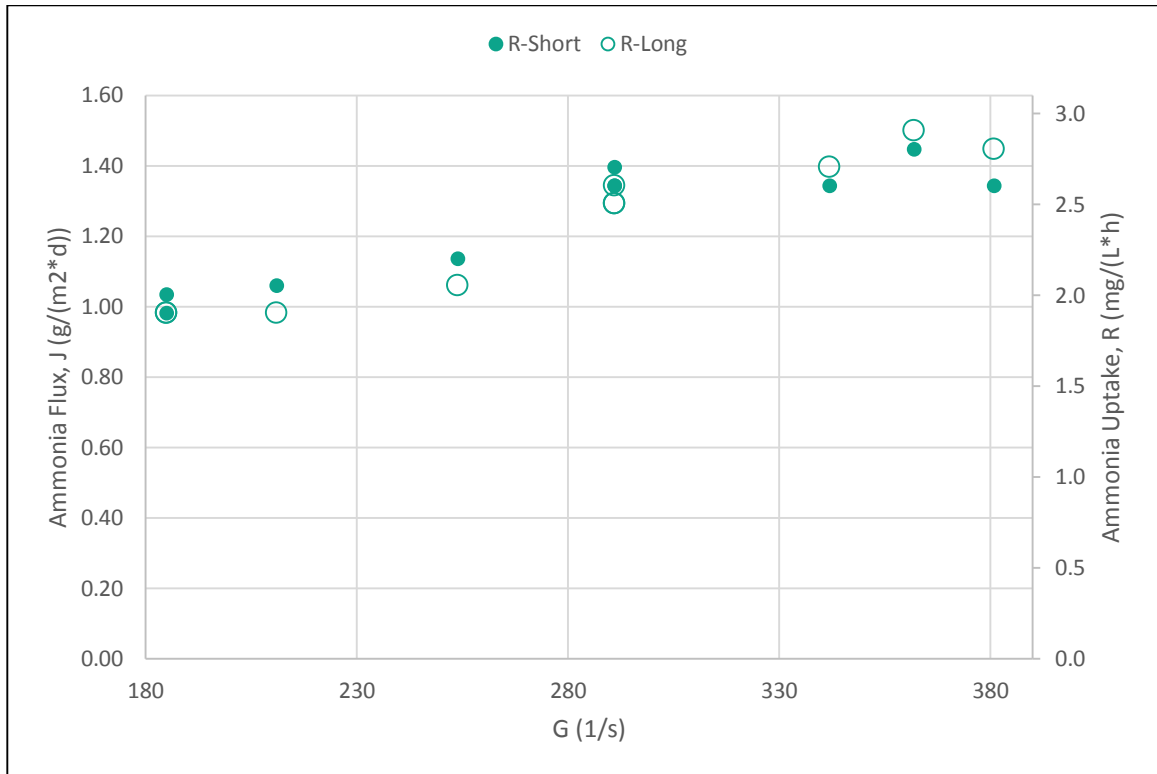
Figure 20 – Batch test nitrate production by R-Short and R-Long (NOB Activity).

	J Range	J Avg.	k Avg.	k Std. Dev.
Table 5 - Summary of Flux and K Values				
	(g/(m²•d))	(g/(m²•d))	(g/(m²•d))	(g/(m²•d))
R-Short	2.43-3.15	2.93	3.11	0.23
R-Long	1.92-3.16	2.68	2.81	0.14

Variability along media length

Differences in biofilm mass and activity along the length of media were quantified by

sectioning the R-Long media into thirds, which were divided into "middle" and "end"

sections for further analyses. During the steady state period of biofilm mass (after day

59, Figure 16), the R-long end sections had on average of 0.134 mg VBS/cm2, or 27%

more biomass than the middle sections, which was a statistically significant difference (p

< 0.01) (Figure 21). The greater concentration of biomass on the outer portions of the

MBBR media was consistent with a previous report (Bjornberg et al. 2009), and may

have been due to lower substrate (ammonia or oxygen) concentrations in the media

interior.

Batch tests were done of the media sections with added ammonia (to test AOB activity)

and nitrite (to test NOB activity), and an equal area quantity of R-short media was tested

as well for comparison. Ammonia uptake by the end and middle R-Long sections, and

also the R-short media were nearly identical (Figure 22), with an average flux over the

one hour test of 3.15 g/(m2*d). The end test ammonia concentration was

approximately 27 mg NH_4-N/L.

This suggests that the AOB activity was distributed fairly evenly along the length of the

R-Long media, and that these were also similar to the R-short media, despite differences

in the biofilm quantities for the three biofilm sources (Figure 21). However, the nitrate

production by the R-Long end section flux rates were consistently greater than R-Long

mid sections and R-Short sections, and the R-Long mid sections had a flux rate slightly

higher than the R-short media (Figure 23). The average end test nitrite concentration was 37 mg NO_2-N/L.

These results suggest the NOB activity was more concentrated towards the ends of the media, which may have been linked to the larger quantity of biomass on the media ends (Figure 21). Bjornberg et al. 2009 suggested that a thicker media edge biofilm would be dominantly responsible for nutrient removal and that the inner interior biofilm is thought to be performing at minimal activity. While AOB activity was evenly distributed along the length of R-Long media, which is inconsistent with Bjornberg et al. 2009 findings, the NOB activity being more significant in the media edge biofilm is somewhat consistent. However, the R-Long media interior biofilm was still performing at comparable NOB flux rates to edges which suggests that the NOB activity was not as minimal as previously thought. This may be attributed to a lack of seasonal temperature variation in R-Short and R-Long as well as a synthetic feed absent of reduced carbon to discourage heterotrophic growth.
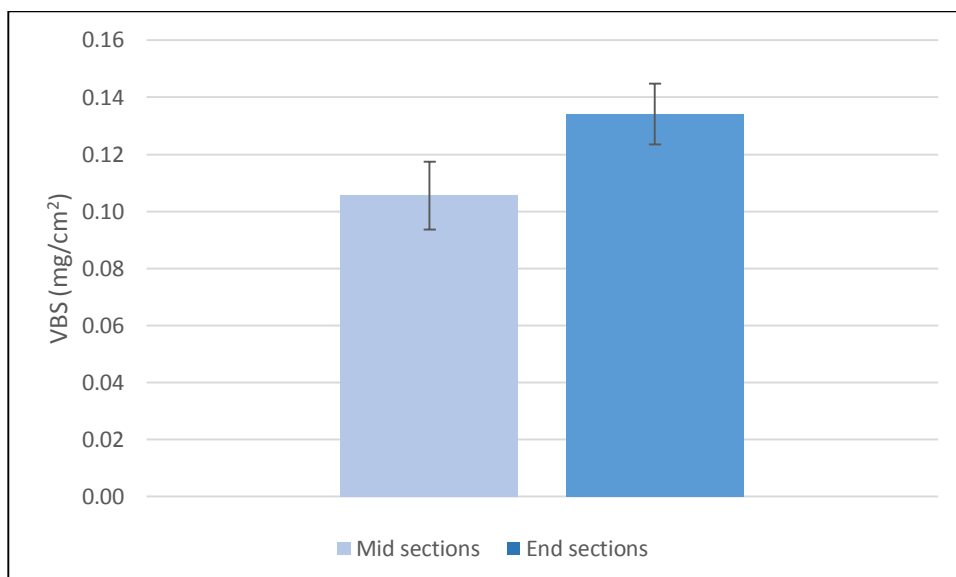
Figure 21 – Average volatile biofilm solids along the length of R-Long media; error bars show VBS standard deviation.
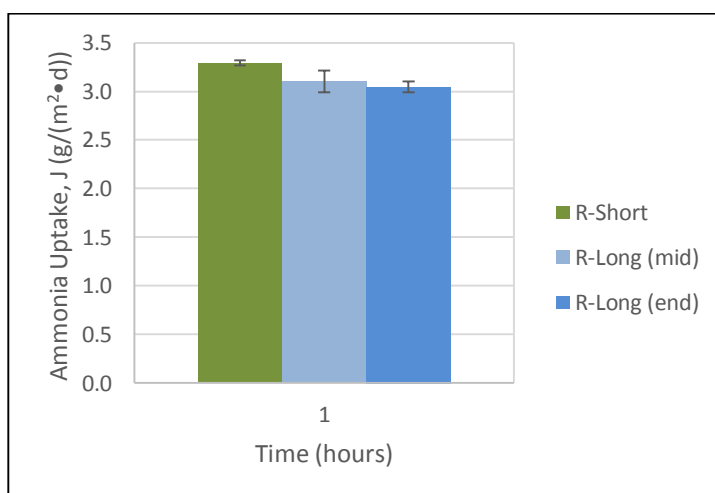
Figure 22 – Ammonia consumption during small scale batch test; similar performance was observed; error bars show ranges.
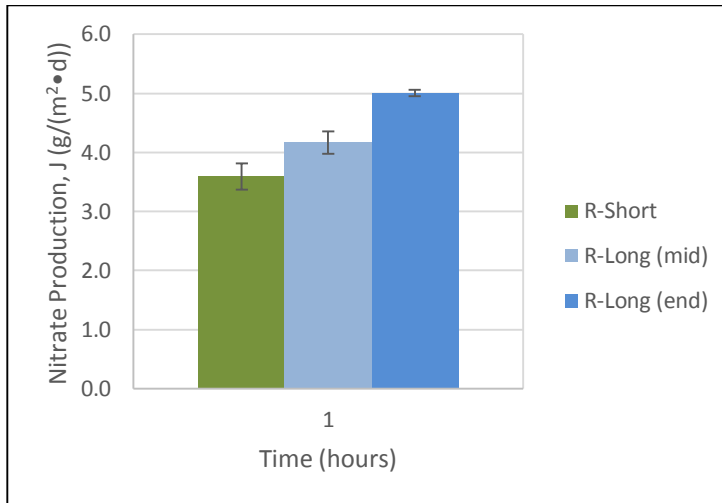
Figure 23 – Nitrate production in small scale batch test; end sections have the greatest NOB activity; error bars show ranges of duplicate tests.

Shock Loading Inhibition

A series of batch tests was performed with the same starting ammonia concentrations as in variable G batch testing (30 mg N/L) for control and an increased starting concentration of ammonia (60 mg N/L) to test the differences in activity between R-Long and R-Short and elucidate inhibition effects. Figure 24 demonstrates little to no effect of increased FA on AOB activity. The 30 mg NH_4-N/L and 60 mg NH_4-N/L tests resulted in similar ammonia uptake of each individual reactor at all three G values tested. However, the NOB activity was reduced significantly in R-Short for each G value (RS 60 values compared to RS 30 values, Figure 24),and was an average of 0.54 g/(m2•d) less than for the higher ammonia test, while R-Long NOB activity was affected very little

at higher FA concentrations (Figure 25). R-Short NOB performance resulted in 36% FA inhibition on average from low to high G values while R-Long only experienced 4% inhibition.

These results demonstrate the greater resilience by NOBs to inhibition in the thicker, more protected biofilm of R-Long. While the extra biomass does not have greater nitrification performance in normal operating conditions, the tolerance of higher FA levels in R-Long suggests a more robust biofilm capable of handling abrupt changes in FA concentrations. Park et al., 2009 determined that at FA concentrations as low as 0.64 mg NH_3-N/L can induce inhibition effects of NOB. During the 60 mg NH_4-N/L batch testing at pH 7.25 where FA was approximately 0.6 mg NH_3-N/L, the inhibition response is observable but is more substantial in R-Short (Figure 25).

Figure 24 – AOB activity of R-Short and R-Long during 30 mg N/L and 60 mg N/L batch tests; error bars show ranges.
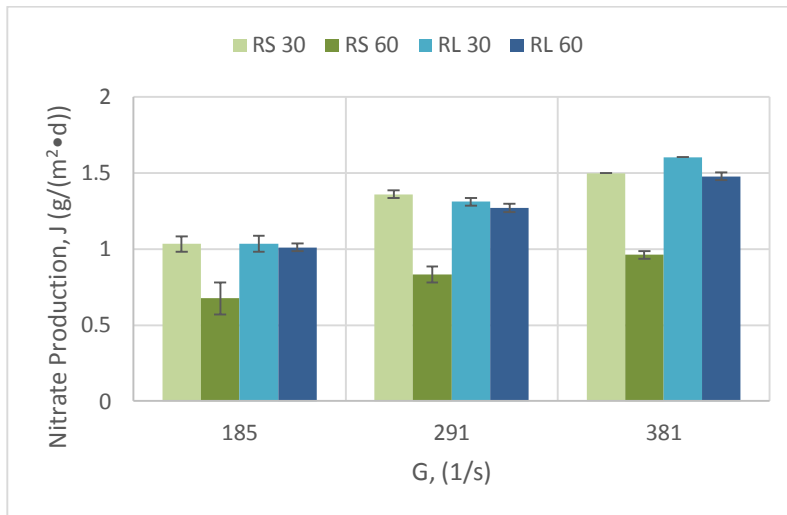
Figure 25 – NOB activity of R-Short and R-Long during 30 mg N/L and 60 mg N/L batch tests; error bars show ranges.

pH Inhibition

After observing effects of inhibition on NOBs by FA, pH change was studied through another series of batch tests. High pH 8.50 and low pH 6.00 batch tests were conducted with added ammonia and nitrite to observe effects of pH induced speciation of substrates. High pH batch tests resulted in an increase of unionized ammonia (ammonium pK_a = 9.25) while the low pH batch tests increased concentrations of nitrous acid (nitrous acid pK_a = 3.40).

The results shown in Figure 26 demonstrate the effect of FNA inhibition on AOB in R-Short and R-Long. From neutral pH 7.25 to low pH 6.00, there was an effect of 49%

inhibition for R-Short and 48% inhibition for R-Long. This similar flux rate reduction in each reactor further suggests the uniform distribution of AOB along both media types and suggests that neither is more protected in the biofilm despite the longer media having a lower internal flow velocity than the shorter media. At higher pH the flux rate for ammonia utilization increased by 13% for R-Short and 21% for R-Long. This is attributed to lower concentrations of FNA at higher pH resulting in a very low inhibition effect on AOB.

Effects of pH on NOB activity are shown in Figure 27. Nitratation rates were consistently greater in R-Long than R-Short for all pH values. This is attributed to the greater free ammonia concentrations in this series of batch tests affecting R-Short more than R-Long. Continuous operation free ammonia concentrations were not inhibiting which is why the same effect isn't observed at steady state conditions. From neutral pH 7.25 to high pH 8.50, R-Short had a substantial inhibition effect of 76% while R-Long only exhibited 14% inhibition. The thicker biofilm in R-Long therefore appeared to provide greater protection to the NOB to NH3 than the thinner R-Short biofilm. At low pH 6.00 the NOB in both systems had higher nitratation flux rates than at neutral pH 7.25 due to the near absence of FA. See Table 6 for calculated amounts of FA per total ammonia species at pH values in the range of this batch test series.

Since NOB sensitivity to FA inhibitionwas apparent, MBBR systems with shorter media like R-Short would be more favorable in very stable (stable pH and influent ammonia loading rates) full scale systems or full scale shortcut biological nitrogen removal

processes. These processes such as ANAMMOX and SHARON require nitrite

accumulation to be successful in nitrogen removal and to achieve this nitrite

accumulation the NOB activity needs to be completely suppressed; this can be achieved

with high FA concentrations (He et al., 2012; Hellinga et al., 1998; Park et al., 2010).
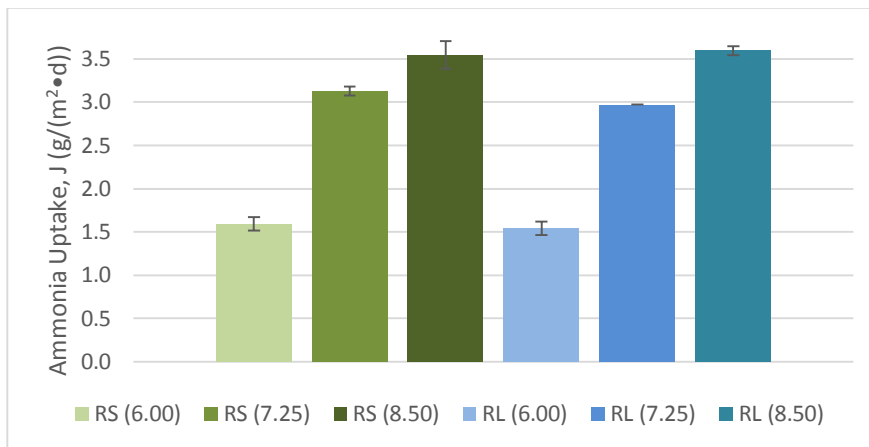
Figure 26 – AOB activity during variable pH batch tests; error bars show ranges.
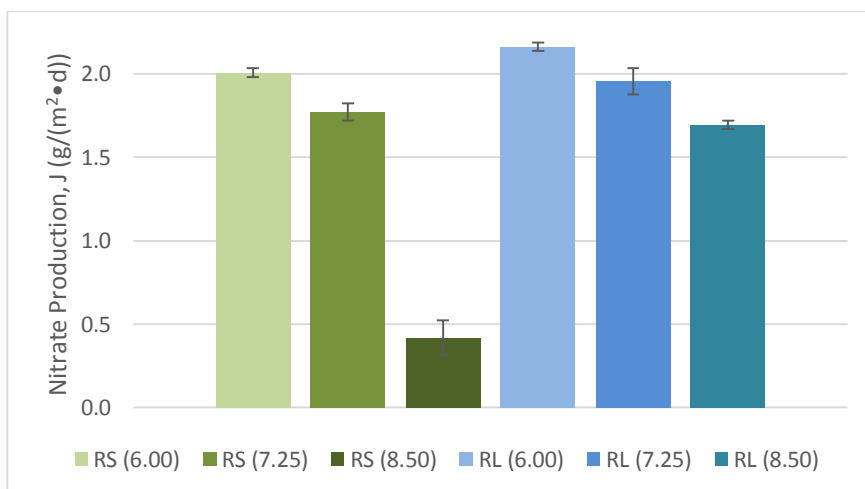
Figure 27 – NOB activity during variable pH batch tests; error bars show ranges.

Table 6 – Calculated Ammonia and Nitrous Acid Speciation		
pH	[NH3]/[NH4+] %	[HNO2]/[NO2-]
6	0.1%	0.3%
6.5	0.2%	0.1%
7	0.6%	0.0%
7.5	1.8%	0.0%
8	5.6%	0.0%
8.5	17.8%	0.0%

To ensure that inhibition effects were being driven by chemical speciation, rather than simply pH, a series of batch tests was performed without any starting FA for NOB while another series of tests was conducted without any starting FNA for AOB.

The AOB activity results are shown in Figure 28. Starting the batch test with no nitrite kept FNA close to zero at neutral and low pH for the duration of the test. Some nitrite was produced during the test but concentrations were low enough to prevent significant FNA accumulation. Also worth noting are the ammonia flux rates for this test

of near 3 g/(m2•d) (Figure 28) were similar to the flux rates at neutral pH where ammonia and nitrite were both added (Figure 26).

NOB activity was notably lower at pH 8.50 during the batch test series with no starting ammonia (Figure 29). Again, R-Long nitratation rates were consistently greater than R-Short nitratation rates across all pH values as in the previous test with starting ammonia and nitrite. The flux rates in this test series were near double the flux rates for the pH 7.25 tests with added ammonia and nitrite (Figure 27) which suggests that FA was the dominant cause of inhibition at higher pH, with even slight inhibition at neutral pH.
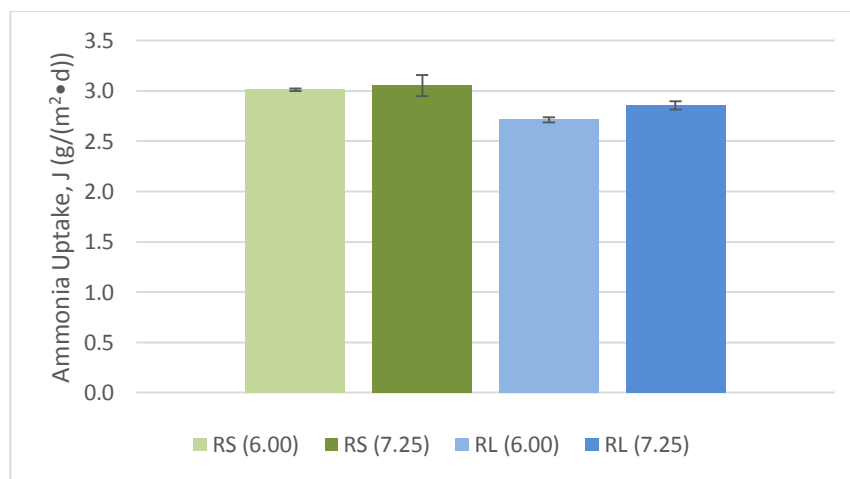
Figure 28 – AOB activity during low and neutral pH batch tests without added FNA; error bars show ranges.
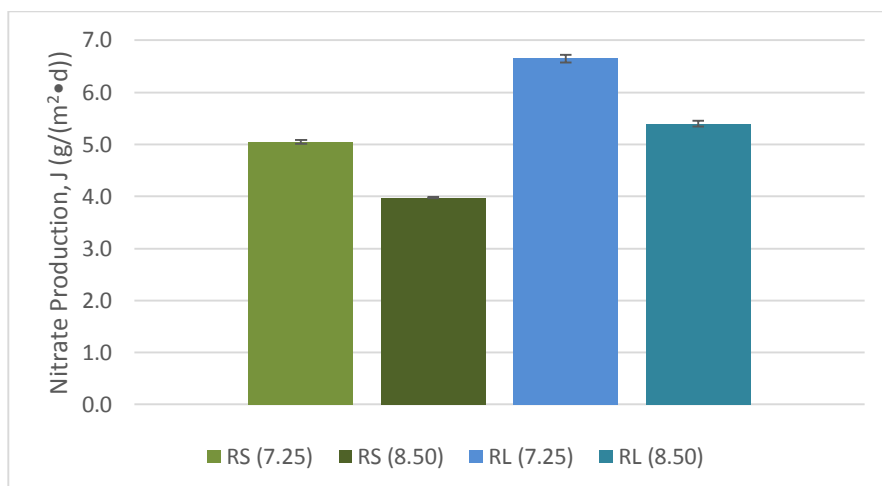
Figure 29 – NOB activity during low and neutral pH batch tests without added FA; error bars show ranges.

CHAPTER 5 CONCLUSIONS

To our knowledge, this study has provided the first evaluation of nitrification in MBBR systems with media size (length) being the primary independent variable rather than morphology or specific area of carriers. With a startup time of about 100 days, MBBR systems are relatively quick to upgrade and retrofit into an existing municipal wastewater treatment plant. The following conclusions can be drawn from this study:

1. Media of different length have similar performance in a continuous MBBR system assuming low (but not limiting) effluent ammonia and near neutral pH. Shorter media has a greater performance on a per biomass basis which may be more desirable for full scale operation due to the shorter startup time of growing less biomass.

2. Shorter media have greater nitrification rates at low to mid range G values. High range G values render media length irrelevant to nitrification rates. This is due to an increased internal flow velocity causing substrate concentration along the length of the media to approach the bulk solution concentration. This effect is not as significant in shorter media which may be the reason for the difference in performance at low to mid range G values. Shorter media may be more energy efficient for full scale systems aerating/mixing at low to mid range G values.

3. More biomass attachment on the inner edges of media is correlated with higher NOB activity. Inner edges and inner interior, although variable in mass, have similar AOB activity suggesting a more uniform distribution of AOB along media length.

4. The biofilms grown on different length media responded differently to inhibition. They exhibited similar responses to FNA inhibition of AOB, but biofilms grown on longer media are more tolerant to FA inhibition of NOB, suggesting that longer or more protected media may aid in preventing inhibition of nitrification. Biofilms grown on shorter media may be more favorable in full scale implementation for systems that have little variation in influent concentrations and pH change; additionally shorter media biofilms are more favorable for nitrite accumulation in shortcut biological nitrogen removal processes such as ANAMMOX or SHARON due to their inherent sensitivity to FNA inhibition of NOB.

Further research needs include the following:

• Determine the effect of concentration along the length of the media approaching bulk media concentration as mixing intensity increases the advective flow through media.

• Determine whether these inhibition result are consistent with other inhibitors.

• Determine effectiveness of shorter media implemenation in shortcut biological nitrogen removal systems or for other nitrite accumulation purposes.

REFERENCES

American Public Health Association, American Water Works Association, Water Environment Federation (2012). Standard Methods for the Examination of Water and Wastewater, 22nd Edition. American Water Works Association, Washington, D.C.

Anthonisen, A.C., Loehr, R.C., Prakasam, T.B.S., Srinath, E.G., 1976. Inhibition of nitrification by ammonia and nitrous acid. Water Environment Federation 48 (5), 835-852.

Bjornberg, C., Lin, W., and Zimmerman, R., 2009. Effect of temperature on biofilm growth dynamics and nitrification kinetics in a full-scale MBBR system. Proceedings of the WEFTEC Conference. Water Environment Federation, Alexandria, Va.

Boltz, J.P., Morgenroth, E., Sen, D., 2010. Mathematical modelling of biofilms and biofilm reactors for engineering design. Water Science and Technology 62 (1), 1821-1836.

Chung, J., Bae, W., Lee, Y.W., Rittmann, B.E., 2007. Shortcut biological nitrogen removal in hybrid biofilm/suspended growth reactors. Process Biochemistry 42 (1), 320-328.

Eberl, H., Morgenroth, E., Noguera, D., Picioreanu, C., Rittmann, B., van Loosdrecht, M., and Wanner, O., (2006). Mathematical Modeling of Biofilms. Scientific and TechnicalReport No. 18, IWA Publishing: London, England.

He, Y., Wendong, T., Ziyuan, W., Walid, S., 2012. Effects of pH and seasonal temperature variation on simultaneous partial nitrification and anammox in free-water surface wetlands. Journal of Environmental Management 110 (1), 103-109.

Hellinga C., Schellen A.A.J.C., Mulder J.W., van Loosdrecht M.C.M., Heijnen J.J., 1998. The SHARON process: an innovative method for nitrogen removal from ammonium-rich waste water. Water Science and Technology 37 (9), 135–42.

Hem, L.J., Rusten, B. and Ødegaard, H., (1994). Nitrification in a moving-bed biofilm reactor. Water Research 28 (6), 1425–1433.

Henze, M., Van Loosdrecht, M.C.M., Ekama, G.A., and Brdjanovic, D., (2008). Biological Wastewater Treatment: Principles, Modelling, and Design. IWA Publishing, London, England.

Javid, A.H., Hassani, A.H., Ghanbari, B., Yaghmaeian, K., 2013. Feasibility of utilizing movine bed biofilm reactor to upgrade and retrofit municipal wastewater treatment plants. International Journal of Environmental Research 7 (4), 963-972.

Kim, D.J., Ahn, D.H., Lee, D.I., 2005. Effects of free ammonia and dissolved oxygen on nitrification and nitrite accumulation in a biofilm airlift reactor. Journal of Chemical Engineering 22 (1), 85-90.

McQuarrey, J.P., Boltz, J.P., 2011. Moving bed biofilm reactor technology: process applications, design, and performance. Water Environment Research 83 (6), 560-575.

Melcer and Schuler. 2014. Mass Transfer Characteristics of Floating Media in MBBR and IFAS Fixed-Film Systems. Project U4R11 Final Report. Water Environment Research Foundation.

Ødegaard, H., Rusten, B., Westrum, T., 1994. A new moving bed bofilm reactor—applications and results. Water Science and Technology 29 (10–11), 157–165.

Ødegaard, H., Gisvold, B., and Strickland, J., 2000. The influence of carrier size and shape in the moving bed biofilm process. Water Science and Technology 41 (4-5), 383–391.

Ødegaard, H., 2006. Innovations in wastewater treatment: the moving bed biofilm process. Water Science and Technology 53 (9), 17-33.

Okabe S., Satoh H., Watanabe Y., 1999. In situ analysis of nitrifying biofilms as determined by in situ hybridization and the use of microelectrodes. Applied Environmental Microbiology 65 (7), 3182–3191.

Park, S., Bae, W., 2009. Modeling kinetics of ammonium oxidation and nitrite oxidation under simultaneous inhibition by free ammonia and free nitrous acid. Process Biochemistry 44 (1), 631-640.

Park, S., Bae, W., Rittmann, B.E., 2010. Operational boundaries for nitrite accumulation in nitrification based on minimum/maximum substrate concentrations that include effects of oxygen limitation, pH, and free ammonia and free nitrous acid inhibition. Environmental Science and Technology 44 (1), 335-342.

Parker, D.S., (2010). A consultant's perspective on process design for biofilm based wastewater treatment processes in North America. Proceedings of WEF-IWA

Biofilm Reactor Technology 2010 Conference, Portland, Ore., Water Environment

Federation: Alexandria, Va.

Rusten, B., Hem, L.J., and Ødegaard, H., 1995. Nitrification of municipal

wastewater in moving-bed biofilm reactors. Water Environment Research 67 (1), 75–86.

Rusten, B., McCoy, M., Proctor, R. and Siljudalen, J.G., 1998. The innovative

moving bed biofilm reactor/solids contact reaeration process for secondary treatment

of municipal wastewater. Water Environment Research 70 (5), 1083–1089.

Tchobanoglous, G., Franklin L.B., and H.D. Stensel. Wastewater Engineering:

Treatment and Reuse. Boston: McGraw-Hill, 2003. Print.

APPENDIX A DAILY NITROGEN SPECIES MEASUREMENTS

R-Short:

Date	G, 1/s	R-Short effluent NH4	R-Short effluent NO2	R-Short effluent NO3	Influent NH4-N, mg/L	R-Short NH4 Uptake	NO2+NO3	(NO2+NO3)/NH4	Temperature °C
42036	291	27.9	0.5	0.4	19.8	-8.1	0.9	-0.11111	22
42037	291	0.4	0.5	27	21.1	20.7	27.5	1.328502	22
42043	291	18.4	5	15.4	30.6	12.2	20.4	1.672131	22
42046	291	14.3	2.5	7.7	22.8	8.5	10.2	1.2	22
42048	291	10.3	3.7	10.8	22.8	12.5	14.5	1.16	22
42050	291	14.5	4.1	4.7	21.9	7.4	8.8	1.189189	22
42054	291	6.1	8.3	8.7	22.3	16.2	17	1.049383	22
42058	291	4.1	9.7	11.1	23.5	19.4	20.8	1.072165	22
42062	291	9.1	21.4	19.8	48.1	39	41.2	1.05641	22
42067	291	1	5.5	39	41.6	40.6	44.5	1.096059	22
42069	291	1.3	3.9	40	41.6	40.3	43.9	1.08933	22
42072	291	1.5	19	49	62.1	60.6	68	1.122112	22
42074	291	7	45	43	83	76	88	1.157895	22
42078	291	1	47	43	82	81	90	1.111111	22
42081	291	23	63	42	125	102	105	1.029412	22
42084	291	30	62	38	125	95	100	1.052632	22

42086	291	31	61	39	125	94	100	1.063833	22
42089	291	38	84	43	160	122	127	1.040984	22
42095	291	16	130	46	170	154	176	1.142857	22
42100	291	12	133	48	190	178	181	1.016854	22
42104	291	55	129	39	220	165	168	1.018182	22
42107	291	81	116	34	220	139	150	1.079137	22
42112	291	31	120	42	200	169	162	0.95858	22
42117	291	35	130	45	200	165	175	1.060606	22
42121	291	31	135	48	200	169	183	1.08284	22
42126	291	48	120	30	200	152	150	0.986842	22
42129	291	40	115	44	200	160	159	0.99375	22
42132	291	39	109	52	200	161	161	1	22
42135	291	36	97	62	200	164	159	0.969512	22
42138	291	33	90	72	200	167	162	0.97006	22
42141	291	29	89	85	200	171	174	1.017544	22
42143	291	19	85	96	200	181	181	1	22
42146	291	14	83	93	200	186	176	0.946237	22
42150	291	16	93	85	200	184	178	0.967391	22
42154	291	13	95	89	200	187	184	0.983957	22
42157	291	14	90	90	200	186	180	0.967742	22
42160	291	14.5	93	80	200	185.5	173	0.932615	22
42163	291	11.4	93	98	200	188.6	191	1.012725	22
42166	291	13.4	91	97	200	186.6	188	1.007503	22
42169	291	13.8	84	96	200	186.2	180	0.966702	22
42172	291	10.1	84	96	200	189.9	180	0.9478	22

Date	G, 1/s	R-Long effluent	R-Long effluent	R-Long effluent	Influent NH4	R-Long NH4	NO2+NO3	(NO2+NO3)/	Temperature
								67	
42175	291	11.9	82	94	200	188.1	176	0.9356 73	22
42178	291	12.5	83	96	200	187.5	179	0.9546 67	22
42182	291	11	81	96	200	189	177	0.9365 08	22
42186	291	11.5	82	96	200	188.5	178	0.9442 97	22
42190	291	11	80	97	200	189	177	0.9365 08	22
42195	291	13	88	91	200	187	179	0.9572 19	22
42200	291	12.8	88	91	200	187.2	179	0.9561 97	22
42205	291	14.6	84	95	200	185.4	179	0.9654 8	22
42210	291	12.5	88	95	200	187.5	183	0.976	22
42215	291	13.3	89	95	200	186.7	184	0.9855 38	22
42220	291	13.2	89	96	200	186.8	185	0.9903 64	22
42225	291	15.3	84	97	200	184.7	181	0.9799 68	22
42230	291	12	85	97	200	188	182	0.9680 85	22
42235	291	17.9	81	88	200	182.1	169	0.9280 62	22
42240	291	18.2	80	83	200	181.8	163	0.8965 9	22
42245	291	13.1	82	85	200	186.9	167	0.8935 26	22
42250	291	12.6	89	91	200	187.4	180	0.9605 12	22
42255	291	14.4	85	90	200	185.6	175	0.9428 88	22
42260	291	11	83	91	200	189	174	0.9206 35	22
42265	291	13	84	90	200	187	174	0.9304 81	22
42270	291	12.5	85	90	200	187.5	175	0.9333 33	22

R-Long:

Date	G, 1/s	R-Long effluen	R-Long effluen	R-Long effluen	Influen t NH4-	R-Long NH4	NO2+N O3	(NO2+ NO3)/	Tempe rature

		t NH4	t NO2	t NO3	N, mg/L	Uptake		NH4	°C
42036	291	28	0.5	0.3	20.1	-7.9	0.8	-0.10127	22
42037	291	0.3	0.5	20.5	20.8	20.5	21	1.02439	22
42043	291	24.1	5.3	8.4	32.2	8.1	13.7	1.691358	22
42046	291	6.7	7.2	11.5	23.4	16.7	18.7	1.11976	22
42048	291	1.8	4.8	18.8	23.4	21.6	23.6	1.092593	22
42050	291	9.8	4.5	9.3	22.3	12.5	13.8	1.104	22
42054	291	3.9	6.2	13.1	22.3	18.4	19.3	1.048913	22
42058	291	1.5	1.1	17.2	23.1	21.6	18.3	0.847222	22
42062	291	13.5	15	20.4	46.8	33.3	35.4	1.063063	22
42067	291	1.7	6.5	35	41.9	40.2	41.5	1.032338	22
42069	291	1.8	5.3	39	41.9	40.1	44.3	1.104738	22
42072	291	1.9	23	41	61.8	59.9	64	1.068447	22
42074	291	7	38	40	82	75	78	1.04	22
42078	291	0	40	43	82	82	83	1.012195	22
42081	291	20	58	51	125	105	109	1.038095	22
42084	291	12	68	54	125	113	122	1.079646	22
42086	291	10	65	57	125	115	122	1.06087	22
42089	291	16	76	74	160	144	150	1.041667	22
42095	291	10	93	74	170	160	167	1.043735	22
42100	291	11	102	76	190	179	178	0.994413	22
42104	291	59	96	58	220	161	154	0.956522	22
42107	291	65	105	54	220	155	159	1.025806	22
42112	291	28	112	56	200	172	168	0.976744	22

42117	291	35	103	62	200	165	165	1 0.9880	22
42121	291	33	98	67	200	167	165	24 0.9743	22
42126	291	44	90	62	200	156	152	59 1.0189	22
42129	291	42	92	69	200	158	161	87	22
42132	291	34	93	73	200	166	166	1 0.9651	22
42135	291	28	93	73	200	172	166	16 0.9606	22
42138	291	22	93	78	200	178	171	74 0.9888	22
42141	291	21	95	82	200	179	177	27 0.9945	22
42143	291	16	94	89	200	184	183	65 0.9456	22
42146	291	16	95	79	200	184	174	52 0.9945	22
42150	291	15	107	77	200	185	184	95 0.9787	22
42154	291	12	105	79	200	188	184	23 0.9523	22
42157	291	11	100	80	200	189	180	81 0.9536	22
42160	291	10.2	98	83	200	189.8	181	35 0.9682	22
42163	291	11	82	101	200	189	183	54 0.9541	22
42166	291	12.4	84	95	200	187.6	179	58 0.9388	22
42169	291	10.4	86	92	200	189.6	178	19 0.9617	22
42172	291	11.8	92	89	200	188.2	181	43 0.9496	22
42175	291	11.5	94	85	200	188.5	179	02 0.9622	22
42178	291	11.9	95	86	200	188.1	181	54 0.9627	22
42182	291	12	96	85	200	188	181	66 0.9531	22
42186	291	12.2	94	85	200	187.8	179	42 0.9564	22
42190	291	11.8	96	84	200	188.2	180	29 0.9508	22
42195	291	14.9	89	87	200	185.1	176	37	22
42200	291	13	92	89	200	187	181	0.9679	22

								14	
42205	291	10.5	90	88	200	189.5	178	0.9393 14	22
42210	291	12.8	91	88	200	187.2	179	0.9561 97	22
42215	291	11.3	92	88	200	188.7	180	0.9538 95	22
42220	291	12.5	92	87	200	187.5	179	0.9546 67	22
42225	291	15	92	86	200	185	178	0.9621 62	22
42230	291	12.8	93	88	200	187.2	181	0.9668 8	22
42235	291	16.5	88	81	200	183.5	169	0.9209 81	22
42240	291	17	87	85	200	183	172	0.9398 91	22
42245	291	12	90	91	200	188	181	0.9627 66	22
42250	291	12.1	90	90	200	187.9	180	0.9579 56	22
42255	291	14	89	91	200	186	180	0.9677 42	22
42260	291	11.7	92	89	200	188.3	181	0.9612 32	22
42265	291	11.6	90	89	200	188.4	179	0.9501 06	22
42270	291	11.8	90	90	200	188.2	180	0.9564 29	22

APPENDIX B BIOMASS MEASUREMENTS

R-Short:

Date	Reactor	Sample	[SHORT] R3 TSS (mg/L)	R-Short	TSS per SA (mg/cm^2)	R 3 [SHORT] VBS per SA (mg/cm^2)
42037	R3 & R4	Time Zero fluid sample of PE and A/S	1910	1520	NA	NA
42044	R3	SF	2	2	NA	NA
42044	R3	10 media	21.25523	12.75314	0.044551	0.026731
42053	R3	12 media	14.13529	14.13529	0.029701	0.029701
42060	R3	12 media	14.09344	14.09344	0.029701	0.029701
42067	R3	12 media	17.5645	17.5645	0.037126	0.037126
42074	R3	12 media	21.01464	21.01464	0.044551	0.044551
42081	R3	12 media	20.95188	20.95188	0.044551	0.044551

42088	R3	12 media	59.18584	38.29672	0.126229	0.081678
42095	R3	12 media	62.47908	55.53696	0.133654	0.118804
42121	R3	12 media	107.2786	107.2786	0.230182	0.230182
42132	R3	12 media	103.5042	89.70363	0.222757	0.193056
42146	R3	12 media	106.6301	92.87134	0.230182	0.200481
42157	R3	12 media	113.1642	99.44735	0.245033	0.215332
42178	R3	12 media	116.2378	109.4003	0.252458	0.237607
42185	R3	12 media	119.2904	109.0656	0.259883	0.237607
42215	R3	12 media	125.72	101.9351	0.274733	0.222757
42245	R3	12 media	125.333	94.84658	0.274733	0.207906
42275	R3	12 media	135.0767	111.4383	0.297009	0.245033

R-Long:

Date	Reactor	Sample	[LONG] R4 TSS (mg/L)	R-Long	TSS per SA (mg/cm^2)	R4 [LONG] VBS per SA (mg/cm^2)
42037	R3 & R4	Time Zero fluid sample of PE and A/S	1910	1520	NA	NA
42044	R4	SF	10	10	NA	NA
42044	R4	5 media	28.34728	25.51255	0.059404	0.053463
42053	R4	4 media	24.71234	24.71234	0.051978	0.051978
42060	R4	4 media	28.159	28.159	0.059404	0.059404
42067	R4	4 media	31.58473	31.58473	0.066829	0.066829
42074	R4	4 media	34.98954	34.98954	0.074254	0.074254
42081	R4	4 media	48.83891	48.83891	0.103956	0.103956
42088	R4	4 media	142.5994	93.9069	0.304443	0.200487
42095	R4	4 media	187.249	180.3138	0.400974	0.386123
42112	R4	4 media	203.9697	179.7699	0.438101	0.386123
42126	R4	4 media	186.1192	186.1192	0.400974	0.400974
42143	R4	4 media	188.9906	182.1182	0.4084	0.393549
42160	R4	4 media	219.2469	188.4153	0.475229	0.4084

42178	R4	4 media	249.3149	187.84	0.542058	0.4084
42185	R4	4 media	204.2887	190.6695	0.445527	0.415825
42215	R4	4 media	227.4215	183.295	0.497505	0.400974
42245	R4	4 media	206.4174	186.114	0.452952	0.4084
42275	R4	4 media	192.2856	192.2856	0.423251	0.423251

APPENDIX C NUTRIENT FEED AND WATER FEED CALCULATIONS

Volume of Reactor (L)	10.53
Q Nutrient Feed (mL/min)	2.20
Q H20 Feed (mL/min)	4.80
Q Total (mL/min)	7.00
Q Total (L/hr)	0.42
HRT (hr)	25.07
Variable NH4-N Concentration (R3,R4)	
Desired NH4-N Concentraiton in Influent (mg/L)	200.00
Concentration of NH4-N 20L Carboy Feed (mg/L)	636.36
Mass of NH4-N In 20L Carboy (g)	12.73
Mass of NH4-Cl add to 20L to obtain Desired Concentration (g)	48.63

Nutrient Feed	Influent Feed (mg/L)	Nuetrient Feed (mg/L)	Mass Added to 20L (g)
NH4Cl	variable	variable	variable
KH2PO4	100.000	318.182	6.364
NaHCO3	350.000	1113.636	22.273
EDTA	6.600	21.000	0.420
Trace Metals			Mass Added to 2L stock Solution (g)

FeSO4-7H2O	5.000	15.909	0.795	31.818
CuSO4-5H2O	0.120	0.382	0.019	0.764
NaMoO4	0.003	0.008	0.0004	0.016
Water Feed (Separate from nuetrient feed)				
Fill 50L Carboy With Tap Water (Approx Residual Cl2 of 1mg/L) 1.5 mg/L NaHSO3per mg/L Cl2removed, 75mg NaHSO3/50L H2O feed After Adding 75 mg NaHSO3, Bubble with Airstone overnight then add…				
CaCl2	16.000	23.333	1.167	
MgSO4	19.510	28.452	1.423	